
Signature Placement in Post-Quantum TLS Certificate Hierarchies: An Experimental Study of ML-DSA and SLH-DSA in TLS 1.3 Authentication

José Luis Delgado

Universitat Oberta de Catalunya
jdelgado13@uoc.edu

Abstract

Post-quantum migration in TLS 1.3 should not be understood as a flat substitution problem in which one signature algorithm is replaced by another and the resulting deployment cost is read directly from primitive-level benchmarks. In certificate-based authentication, the practical effect of a signature family depends on where it appears in the certification hierarchy, how much of that hierarchy is exposed during the handshake, and how the resulting cryptographic burden is distributed across client and server roles. This makes post-quantum TLS migration a problem of cryptographic design in authenticated key establishment, rather than merely a matter of algorithm selection [10, 5, 4, 6].

This paper presents a local experimental study of TLS 1.3 authentication strategies built on OpenSSL 3 and oqsprovider. Using a reproducible laboratory, it compares ML-DSA and SLH-DSA across multiple certificate placements, hierarchy depths, and key-exchange modes, including classical, hybrid, and pure post-quantum configurations. The analysis is organized around four complementary campaigns: a leaf-only comparison, a full hierarchy strategy matrix, a depth comparison, and a key-exchange exploration [7, 8, 11, 9].

Across the experimental matrix, the clearest discontinuity appears when SLH-DSA is placed in the server leaf certificate. In that configuration, handshake latency and server-side compute cost increase by orders of magnitude, while strategies that confine SLH-DSA to upper trust layers and preserve ML-DSA in the interactive leaf remain within a substantially more plausible operational range. The results further show that transport size alone does not explain the heavy regime: outside leaf-SLH scenarios, transferred bytes and observed chain size track latency closely, but once SLH-DSA reaches the leaf, server-side cryptographic cost becomes dominant [11, 9, 3].

The paper therefore argues that post-quantum TLS migration is best evaluated as a problem of certificate-hierarchy design, chain exposure, and cryptographic cost concentration during live authentication. In practical terms, signature placement matters at least as much as signature-family choice.

Keywords: TLS 1.3, post-quantum cryptography, post-quantum authentication, ML-DSA, SLH-DSA, ML-KEM, certificate hierarchies, X.509, PKI, authenticated key establishment.

Contents

1	Introduction	5
1.1	Post-quantum migration in TLS as a cryptographic design problem	5
1.2	Why signature placement matters	5
1.3	Research gap	5
1.4	Research questions and thesis	6
1.5	Contributions	6
1.6	Paper organization	7
2	Cryptographic and Protocol Background	7
2.1	TLS 1.3 certificate authentication and chain transmission	7
2.2	Post-quantum signature standardization: ML-DSA and SLH-DSA	7
2.3	Hybrid transition logic and deployment tension	8
2.4	Placement, exposure, and operational cost	8
3	Related Work	8
3.1	Prior work on post-quantum TLS and hybrid handshakes	8
3.2	Prior work on certificate overhead and chain-related cost	9
3.3	Positioning of this paper	9
4	Research Questions and Study Scope	10
4.1	Research questions	10
4.2	Scope and non-goals	10
5	Experimental Methodology	11
5.1	Experimental objective	11
5.2	Implementation stack and execution environment	11
5.3	Scenario construction	11
5.4	Measurement model	12
5.5	Experimental campaigns	12
5.6	Metric semantics and normalization	13
5.7	Methodological cautions	13
6	Results	14
6.1	Global performance landscape	14
6.2	Campaign A: leaf-only comparison	15
6.2.1	Classical KEX	16
6.2.2	Hybrid KEX	16
6.2.3	Main result of Campaign A	17
6.3	Campaign B: full hierarchy strategy matrix	17
6.3.1	Fully-ML baseline	18

6.3.2	Root-SLH with ML leaf	18
6.3.3	Leaf-SLH strategies	18
6.3.4	Main result of Campaign B	19
6.4	Campaign C: depth comparison	19
6.4.1	All-ML families	19
6.4.2	Root-SLH with ML leaf	19
6.4.3	Leaf-SLH families	20
6.4.4	Main result of Campaign C	21
6.5	Campaign D: KEX mode exploration	21
6.5.1	Main result of Campaign D	22
7	Cross-Cutting Cryptographic Interpretation	22
7.1	Signature placement versus mere signature presence	22
7.2	Transport-related overhead versus cryptographic cost	23
7.3	Effective chain exposure as a first-class variable	25
7.4	Emergence of a distinct leaf-SLH regime	26
8	Client/Server Cost Decomposition	26
8.1	Why client-only observations were insufficient	26
8.2	Balanced regime in all-ML scenarios	27
8.3	Validation-skewed regime in upper-layer SLH scenarios	28
8.4	Overwhelmingly server-bound regime in leaf-SLH scenarios	28
8.5	Supporting microarchitectural signals	30
9	Operational Implications for PQ TLS Deployment	30
9.1	From server-side handshake cost to service capacity	31
9.2	Capacity loss under leaf-SLH	31
9.3	Cost-per-million-handshakes interpretation	32
9.4	Service-class translation	33
9.5	Operational plausibility of hierarchy strategies	34
10	Threats to Validity and Limitations	35
10.1	Local execution environment	35
10.2	Single implementation stack	35
10.3	Semantics of observed chain exposure	36
10.4	Perf as proxy rather than full function tracing	37
10.5	Economic model as derived interpretation	37
11	Conclusion	38
11.1	Main finding	38
11.2	Implications for certificate hierarchy design	38

11.3	What remains open	38
11.4	Final closing statement	39
A	Scenario Inventory	40
B	Additional Measurement Notes	42
B.1	Observed chain length versus logical hierarchy depth	42
B.2	Semantics of <code>served_chain_der_bytes</code>	42
B.3	Scenario reuse and deduplication	42
B.4	Non-uniform sample sizes	42
B.5	Use of perf-derived metrics	42

1 Introduction

1.1 Post-quantum migration in TLS as a cryptographic design problem

TLS 1.3 is a cryptographic protocol for authenticated key establishment, not a neutral container into which one may insert stronger primitives without materially changing the structure of the authentication path. In certificate-based deployments, the authentication phase is mediated by X.509 chains, signature verification, chain transmission, and the timing constraints of an interactive handshake. As a result, post-quantum migration in TLS cannot be reduced to a flat algorithm swap in which a classical signature is replaced by a post-quantum one and the deployment problem is considered solved [10, 11].

This point has become more pressing after the publication of NIST’s first final post-quantum standards, including ML-KEM for key establishment, ML-DSA for digital signatures, and SLH-DSA as a stateless hash-based signature standard [5, 4, 6]. These standards provide the cryptographic basis for migration, but they do not eliminate the deployment question. In TLS, signature schemes are not consumed in the abstract. They are instantiated through certificate hierarchies, exposed through specific handshake messages, and processed under latency-sensitive client/server interaction. The migration problem is therefore cryptographic in a protocol-and-PKI sense, not merely algorithmic in a primitive-selection sense.

Accordingly, the relevant design question is not only which post-quantum signature family is acceptable in principle, but which placements remain viable once live TLS authentication is measured as an end-to-end cryptographic event. In that setting, certificate-hierarchy design becomes part of the security engineering problem itself.

1.2 Why signature placement matters

The practical cost of a signature family in TLS depends not only on its intrinsic size or verification complexity, but also on where it appears in the certificate hierarchy. A signature placed in a long-lived trust anchor does not necessarily have the same operational meaning as the same family placed in the server leaf certificate that is exposed directly in the interactive handshake. This distinction is easy to blur in high-level discussions of post-quantum migration, but it is decisive in deployment.

In TLS 1.3, the server certificate and the transmitted certificate chain participate directly in the authenticated portion of the handshake [10]. For that reason, the leaf certificate occupies a special position. It is the point at which certificate design, signature verification, and server-side authentication cost become inseparable from interactive protocol behavior. By contrast, signatures placed in upper trust layers may still influence validation burden, chain size, and transmitted material, but they need not impose the same live authentication cost profile.

This suggests that post-quantum authentication should not be studied only through primitive-level benchmarks or certificate-size comparisons. It should also be studied through hierarchy-sensitive placement strategies. In particular, there is strong reason to distinguish between scenarios in which a heavier signature family is confined to upper trust layers and scenarios in which that same family reaches the handshake-exposed server leaf.

1.3 Research gap

Existing work has already shown that post-quantum authentication in TLS can introduce substantial overhead, and that certificate-related effects matter in practice [11]. Other work has explored mixed certificate chains as a migration strategy for post-quantum TLS authentication, thereby making clear that transitional hierarchies deserve explicit study rather than being treated as temporary implementation clutter [9]. More recent evaluation frameworks have also expanded the measurement space for post-quantum TLS by examining classical, hybrid, and pure post-quantum configurations in controlled experimental settings [3].

However, the literature still leaves an important gap. Prior studies have tended to emphasize one or more of the following: primitive-level overhead, certificate-size growth, hybrid key exchange, or general TLS performance under post-quantum integration. Much less attention has been devoted to a placement-centered question: how the position of a signature family within the certificate hierarchy

shapes the observed chain, the burden visible during the live handshake, and the distribution of cryptographic work across client and server.

That gap matters because placement within the hierarchy is not a cosmetic modeling choice. It affects which certificates are exposed, which signatures are verified in the interactive path, and how cryptographic cost concentrates during real authentication. A transition study that ignores hierarchy-sensitive placement risks collapsing distinct operational regimes into a single flat comparison.

1.4 Research questions and thesis

This paper is organized around the following research questions:

- RQ1. To what extent is the operational cost of TLS 1.3 authentication determined by whether the server leaf certificate uses ML-DSA or SLH-DSA?
- RQ2. Does placing SLH-DSA in upper layers of the certificate hierarchy behave differently from placing it in the leaf exposed to the interactive handshake?
- RQ3. How do chain depth and effective chain transmission affect observed handshake latency and transferred data?
- RQ4. To what extent is the observed degradation explained by transport size, and to what extent by cryptographic processing?
- RQ5. Does moving from classical to hybrid or pure post-quantum key exchange materially change the main migration picture?
- RQ6. What operational implications do these results have for organizations deploying interactive TLS services?

The thesis advanced in this paper is straightforward. The dominant variable is not simply whether ML-DSA or SLH-DSA appears somewhere in the hierarchy, but where it appears. More precisely, the most consequential distinction is not between scenarios in which SLH-DSA is present and scenarios in which it is absent, but between those in which SLH-DSA remains confined to upper trust layers and those in which it reaches the server leaf exposed to the live TLS handshake.

From this follows the paper’s central claim: post-quantum TLS migration is best understood as a cryptographic design problem in certificate hierarchies. Signature placement, effective chain exposure, and client/server cryptographic burden jointly define distinct operational regimes, and the most severe regime is consistently associated with SLH-DSA in the interactive server leaf.

1.5 Contributions

This paper makes the following contributions:

1. It presents a hierarchy-sensitive experimental study of post-quantum TLS 1.3 authentication, centered on certificate placement rather than flat primitive comparison.
2. It evaluates ML-DSA and SLH-DSA across four complementary experimental campaigns that isolate leaf placement, full hierarchy strategy, chain depth, and key-exchange mode.
3. It provides empirical evidence that signature placement has greater explanatory power than mere signature-family presence within the certification hierarchy.
4. It shows that transport expansion alone does not explain the dominant heavy regime observed in leaf-SLH scenarios, even though transport metrics remain highly informative outside that regime.
5. It demonstrates, through client/server performance decomposition, that leaf-SLH scenarios become overwhelmingly server-bound during live TLS authentication.
6. It translates these findings into operational terms, thereby connecting post-quantum certificate-hierarchy design with deployment viability in interactive TLS services.

1.6 Paper organization

The remainder of the paper is organized as follows. Section 2 introduces the cryptographic and protocol background needed to frame post-quantum authentication in TLS 1.3. Section 3 reviews the most relevant prior work and positions the present study within that literature. Section 4 states the research questions more formally and defines the scope of the study. Section 5 presents the experimental methodology, including the implementation stack, scenario construction, measurement model, and metric semantics. Section 6 reports the campaign-level results. Section 7 develops a cross-cutting cryptographic interpretation of those results, with particular attention to signature placement, chain exposure, and the distinction between transport-related and cryptographic cost. Section 8 analyzes client/server workload decomposition. Section 9 translates the measured effects into operational implications for post-quantum TLS deployment. Section 10 discusses threats to validity and limitations. Section 11 concludes.

2 Cryptographic and Protocol Background

2.1 TLS 1.3 certificate authentication and chain transmission

TLS 1.3 provides authenticated key establishment by combining ephemeral key exchange with transcript-bound authentication. In the certificate-based server authentication path, the server transmits a certificate chain in the `Certificate` message and proves possession of the corresponding private key in `CertificateVerify`; both messages are bound to the handshake transcript, which makes certificate handling part of the live cryptographic execution of the protocol rather than a detached PKI afterthought [10].

In Internet deployments, the certificates used in that authentication path typically follow the X.509 profile standardized for PKIX, with a leaf certificate representing the authenticated endpoint and additional certificates conveying the issuing chain needed for validation [1]. For that reason, TLS authentication cost is shaped not only by the negotiated key-establishment mechanism, but also by the structure and contents of the transmitted certificate path. The server leaf occupies a special role in this process: it is the certificate directly associated with the endpoint identity and the key used in the interactive authentication step.

This distinction matters because TLS does not authenticate an abstract signature primitive. It authenticates a concrete endpoint through a concrete certificate path transmitted under protocol timing constraints. As a result, certificate hierarchy, chain exposure, and verification burden may all influence the practical behavior of the handshake. In a post-quantum setting, where signature families can differ sharply in representation size and computational profile, these effects become especially relevant [11, 9].

2.2 Post-quantum signature standardization: ML-DSA and SLH-DSA

NIST’s first final post-quantum standards define ML-KEM for key establishment, ML-DSA for digital signatures, and SLH-DSA as a stateless hash-based digital signature standard [5, 4, 6]. For the purposes of TLS authentication, the most relevant point is not merely that both ML-DSA and SLH-DSA are standardized, but that they instantiate materially different design traditions within post-quantum cryptography.

ML-DSA is a module-lattice-based signature standard derived from the CRYSTALS-Dilithium design lineage and is intended as a general-purpose digital signature mechanism in the post-quantum transition [4]. SLH-DSA, by contrast, is a stateless hash-based standard derived from the SPHINCS+ family and represents a different cryptographic trade-off, one grounded in hash-based security assumptions and stateless tree-based signing [6]. Both are legitimate standardized options, but they need not behave similarly when embedded into certificate hierarchies and exercised inside a live TLS handshake.

That difference should not be overstated at the primitive level beyond what is needed for the present study. This paper does not attempt a full algorithmic comparison of ML-DSA and SLH-DSA in all possible application settings. Its narrower concern is their use in TLS 1.3 certificate authentication, where signature families are not consumed in isolation but as part of transmitted and validated

certification paths. In that setting, standardization establishes cryptographic legitimacy, but not operational equivalence.

2.3 Hybrid transition logic and deployment tension

The transition to post-quantum cryptography is widely understood as a migration problem rather than a single-step replacement event. In TLS, that logic has been especially visible on the key-establishment side, where hybrid designs combine classical and post-quantum components in order to preserve security if at least one constituent remains secure during the transition period [13, 12]. This hybrid reasoning is motivated by compatibility, cryptographic conservatism, and the practical need to move incrementally rather than assume immediate ecosystem-wide convergence [2].

A closely related tension appears in certificate-based authentication. Organizations do not migrate certificate hierarchies in a vacuum. They inherit trust-anchor lifetimes, interoperability constraints, implementation limits, validation behavior, and operational latency budgets. For that reason, the post-quantum transition in TLS is not purely a question of selecting stronger signature primitives. It is also a question of how to stage those primitives across the certification hierarchy and how to control which cryptographic costs are exposed in the live handshake [9, 11].

This is precisely where mixed and hierarchy-sensitive strategies become conceptually important. A deployment may wish to adopt a heavier or more conservative signature family in upper trust layers while preserving a different family at the interactive server leaf, or vice versa. Such choices are not merely administrative PKI details. They are part of the cryptographic transition design itself because they shape how authentication cost is realized under protocol execution.

2.4 Placement, exposure, and operational cost

The central premise of this paper is that certificate placement within the hierarchy is a first-class variable in post-quantum TLS authentication. The relevant question is not only which signature family exists somewhere in the chain, but which certificates are exposed during the handshake and where the corresponding cryptographic burden is paid. Prior work on post-quantum authentication in TLS and on mixed certificate chains already suggests that certificate-related effects can dominate practical overhead and that heterogeneous chains deserve explicit treatment during the transition [11, 9].

This becomes especially important once one distinguishes between logical hierarchy and effective chain exposure. The logical PKI structure may contain roots, intermediates, and leaves, but the set of certificates actually transmitted and processed during the handshake is an empirical property of the deployed authentication path. That effective exposure influences transmitted bytes, validation burden, and potentially the concentration of active work across client and server roles. In other words, chain exposure is not just a representational detail; it is part of the cryptographic cost surface of the protocol.

From that perspective, placement has direct operational meaning. A signature family used in an upper trust layer may influence path validation and chain size, yet still leave the live server authentication step within a bounded cost regime. The same family, when moved into the handshake-exposed leaf, may instead reshape the entire execution profile of the TLS authentication path. The purpose of the present study is to evaluate that distinction systematically by treating hierarchy position, effective chain exposure, and client/server cost concentration as joint variables in post-quantum TLS 1.3 authentication.

3 Related Work

3.1 Prior work on post-quantum TLS and hybrid handshakes

A substantial body of work has already established that TLS is one of the central protocol settings in which post-quantum migration must be evaluated empirically rather than discussed only at the primitive level. In particular, Sikeridis, Kampanakis, and Devetsikiotis studied post-quantum authentication in TLS 1.3 and showed that signature choice can have major consequences for connection-establishment latency and throughput under realistic deployment assumptions [11]. Their work is important not only because it quantifies overhead, but because it makes clear that the authentication

path itself is a serious post-quantum deployment surface rather than a secondary implementation detail.

Subsequent work has expanded the transition picture by examining mixed and hybrid configurations rather than purely uniform post-quantum replacements. In the authentication space, Paul et al. proposed mixed certificate chains for TLS 1.3 as an explicit migration strategy, arguing that different signature algorithms may be assigned to different positions in the same hierarchy in order to balance trust, interoperability, and performance [9]. On the key-establishment side, current IETF work on hybrid key exchange and ML-KEM deployment in TLS reflects the same broader logic: post-quantum migration is being treated as a staged protocol transition in which compatibility and security margins must coexist [13, 12].

The practical experimentation ecosystem has also matured. The Open Quantum Safe project has become a central platform for prototyping post-quantum cryptography in real protocol stacks, including OpenSSL-based TLS deployments through liboqs and oqsprovider [7, 8]. More recent measurement-oriented work, such as the framework of Montenegro et al., has further broadened the empirical basis for post-quantum TLS evaluation by enabling comparative study across classical, hybrid, and pure post-quantum configurations in a unified experimental environment [3]. Taken together, these lines of work have firmly established PQ TLS as a legitimate domain of empirical cryptographic research rather than a merely speculative engineering concern.

3.2 Prior work on certificate overhead and chain-related cost

Within that broader literature, certificate-related overhead has emerged as one of the most consequential sources of deployment cost. Sikeridis et al. already showed that post-quantum authentication in TLS 1.3 cannot be evaluated solely in terms of abstract cryptographic security or primitive-level operation counts, because certificate size, transmitted bytes, and signature verification cost materially affect handshake behavior [11]. Their study therefore helped shift attention from purely algorithmic comparison toward protocol-visible authentication overhead.

Paul et al. pushed this line further by treating the certificate chain itself as a design space rather than as a fixed administrative artifact [9]. Their mixed-chain proposal is especially relevant because it recognizes that post-quantum migration may proceed through heterogeneous hierarchies in which different certificates serve different operational roles. This perspective is crucial for any study that takes PKI structure seriously. It suggests that the effective cost of post-quantum authentication depends not only on which algorithms are chosen, but also on how they are distributed across the hierarchy.

Recent PQ TLS evaluation frameworks have likewise continued to track the relation between cryptographic choices, handshake latency, and protocol overhead [3]. However, even where certificate and size effects are measured, prior work has generally focused on aggregate configuration-level behavior rather than on a placement-centered analysis of certification hierarchies. In other words, the literature has shown that certificates matter, but it has not fully isolated how hierarchy position, effective chain exposure, and client/server cost concentration interact as distinct explanatory variables.

3.3 Positioning of this paper

This paper is positioned deliberately within that gap. It is not a flat benchmark of post-quantum signature algorithms in isolation, and it is not limited to comparing certificate sizes or byte overhead across uniform configurations. It is also not primarily a study of key-exchange substitution, although classical, hybrid, and pure post-quantum KEX modes are included as part of the experimental design. Instead, the central object of study is the certificate hierarchy itself: which signature family is placed at the root, which at the intermediate, which at the server leaf, and how that placement shapes the cost of live TLS authentication.

That positioning distinguishes the present work from prior evaluation efforts in two main ways. First, it treats hierarchy-sensitive signature placement as the principal explanatory variable, rather than as a secondary parameter inside a broader benchmark. Second, it explicitly connects hierarchy placement with effective chain exposure and with client/server workload decomposition during the handshake. In that sense, the paper studies post-quantum TLS authentication not simply as overhead, but as a cryptographic design problem in certificate-path construction and exposure [11, 9, 3].

The resulting contribution is therefore narrower than a general survey of PQ TLS, but more specific in a way that is analytically useful. The paper asks neither which post-quantum primitive is best in the abstract nor which single TLS configuration is globally optimal. It asks which certificate-chain strategies remain operationally plausible once post-quantum signature placement is evaluated where it actually matters: inside the authenticated handshake path of TLS 1.3.

4 Research Questions and Study Scope

4.1 Research questions

The study is organized around six research questions:

- RQ1. To what extent is the operational cost of TLS 1.3 certificate-based authentication determined by whether the server leaf certificate uses ML-DSA or SLH-DSA?
- RQ2. Does placing SLH-DSA in upper layers of the certificate hierarchy behave materially differently from placing it in the handshake-exposed server leaf?
- RQ3. How do hierarchy depth and effective chain exposure shape observed handshake latency and transmitted data during TLS 1.3 authentication?
- RQ4. To what extent is the observed degradation explained by transport-related overhead, and to what extent by cryptographic processing cost?
- RQ5. Does moving from classical to hybrid or pure post-quantum key establishment materially alter the main migration picture?
- RQ6. What operational implications do these results have for organizations deploying interactive TLS services under post-quantum transition constraints?

Taken together, these questions define the paper’s analytical focus. The objective is not to compare signature families in the abstract, but to determine how certificate-hierarchy design shapes the cost of live TLS 1.3 authentication once signature placement, chain exposure, and client/server burden are considered jointly.

4.2 Scope and non-goals

The scope of the paper is deliberately narrow. It studies a concrete cryptographic-operational question: how post-quantum signature placement within TLS 1.3 certificate hierarchies affects the behavior of live certificate-based authentication in a real implementation stack based on OpenSSL 3 and oqsprovider [10, 7, 8]. The goal is therefore not universal prediction across all possible TLS libraries, PKI deployments, or Internet environments, but controlled evaluation of a specific and practically relevant migration problem.

Several non-goals follow from that choice. First, the paper does not claim universality across all implementation stacks. Absolute values may depend on library internals, provider integration, certificate handling behavior, and platform-specific factors. The strongest claims advanced here are therefore structural rather than stack-independent: namely, that hierarchy-sensitive signature placement can decisively shape the operational regime of post-quantum TLS authentication.

Second, the paper does not attempt full internal function tracing or exhaustive microarchitectural attribution. Performance counters are used as regime-level evidence for client/server cost concentration, not as a substitute for complete code-path reconstruction or low-level implementation forensics.

Third, the study does not attempt to measure Internet-wide or WAN-visible latency in arbitrary production conditions. The experiments are conducted in a controlled local environment so that certificate-path effects, chain exposure, and cryptographic cost can be observed with reduced network noise. The resulting latency values should therefore be interpreted as comparative measurements within a real stack, not as direct forecasts of user-perceived latency on the public Internet.

Finally, the paper does not seek to settle the general question of which post-quantum primitive is best in all protocol contexts. Its concern is narrower and more concrete: which certificate-chain strategies remain operationally plausible for TLS 1.3 server authentication when post-quantum signatures are embedded into live X.509-based authentication paths [10, 1, 4, 6]. In that sense, the contribution is

intentionally bounded, but bounded around a problem that is both cryptographically meaningful and operationally consequential.

5 Experimental Methodology

5.1 Experimental objective

The experimental objective of this study is not to benchmark post-quantum signature algorithms in isolation, but to evaluate TLS 1.3 authentication strategies under certificate-hierarchy placements that are meaningful for real deployments. The central concern is therefore cryptographic and protocol-level: how the placement of ML-DSA and SLH-DSA within X.509 certification paths affects the cost of live server authentication during the TLS handshake [10, 1, 4, 6].

Accordingly, the laboratory is designed around hierarchy-sensitive authentication scenarios rather than primitive-level microbenchmarks. The relevant question is not simply whether one signature family is larger or slower in the abstract, but which hierarchy constructions remain operationally plausible once authentication is exercised through a concrete certificate path, transmitted during a real TLS 1.3 handshake, and measured as an end-to-end cryptographic event. This framing is consistent with prior work showing that post-quantum authentication overhead in TLS is shaped by certificate-related effects and should therefore be studied at the protocol level rather than inferred from primitive properties alone [11, 9, 3].

5.2 Implementation stack and execution environment

All experiments were conducted on a local TLS laboratory built around OpenSSL 3 and the Open Quantum Safe provider stack. The cryptographic implementation used `oqsprovider` on top of `liboqs`, thereby enabling access to the post-quantum signature and key-establishment mechanisms required for the study [7, 8]. The signature families of interest were ML-DSA and SLH-DSA, instantiated through concrete algorithm selections appropriate to the chosen security level. On the key-establishment side, the experimental design considered three modes: classical X25519, hybrid X25519MLKEM768, and pure post-quantum MLKEM768 [5, 4, 6, 12, 13].

The server side was driven through `openssl s_server`, parameterized per scenario so as to load the appropriate certificate chain, key material, and TLS group configuration. The client side used a dedicated benchmark client written in C and instrumented specifically for per-handshake measurement. For each run, the client established a fresh TCP connection, forced TLS 1.3, loaded the required provider configuration, selected the key-establishment group for the scenario under test, and executed a full handshake against the server. This design ensured that the unit of observation remained the complete certificate-based authentication event rather than a resumed session or an amortized multi-request connection artifact.

Although earlier exploratory work was carried out in VM-like environments, the final dataset analyzed in this paper was collected on bare metal in order to reduce virtualization-related distortion and to support more reliable server-side performance measurements. This choice is especially important for interpreting the heavy regime associated with leaf-SLH scenarios, where server-side active compute becomes one of the main explanatory variables.

5.3 Scenario construction

The scenario space was defined to isolate hierarchy-sensitive authentication effects. Each scenario is described by a combination of certificate-hierarchy depth, signature-family placement within the hierarchy, and key-establishment mode.

Hierarchy depth was varied between depth 2 and depth 3 configurations. In depth 2 scenarios, the logical certification path consisted of a root and a leaf. In depth 3 scenarios, an intermediate certificate was inserted between root and leaf. This distinction was not introduced merely for administrative completeness. It was necessary in order to study how hierarchy depth interacts with effective chain exposure and with the placement of heavier signature families.

Within each hierarchy, signature families were assigned positionally. The main placement variables are therefore root, intermediate, and leaf. This positional model allows the study to distinguish among

scenarios in which SLH-DSA appears only in upper trust layers, scenarios in which it appears directly in the server leaf, and scenarios in which the entire hierarchy uses a common family. The resulting design makes it possible to ask whether the same signature family has materially different operational meaning depending on where it is embedded in the certification path.

The experimental matrix included both uniform and mixed hierarchies. Uniform hierarchies were used to define the all-ML baseline and selected all-SLH comparison points. Mixed hierarchies were used to evaluate transitional strategies such as root-SLH with ML-DSA preserved in the leaf, as well as heavier placements in which SLH-DSA reaches the interactive certificate. In addition, the key-establishment dimension was varied across classical, hybrid, and pure post-quantum modes in order to determine whether the main picture changes when certificate authentication is combined with different KEX assumptions.

For analysis purposes, the study also defines comparable families of scenarios. These are groups that differ along one principal axis while preserving the rest of the hierarchy structure as far as possible. Examples include leaf-only contrasts under fixed surrounding conditions, depth 2 versus depth 3 comparisons for the same high-level family, and KEX comparisons under comparable chain constructions. This notion of comparability is essential for causal interpretation, since the paper is concerned less with aggregate scenario ranking than with understanding which structural variable governs each observed regime.

5.4 Measurement model

The measurement model is defined at the level of individual handshakes. Each experimental run establishes a fresh TCP connection, performs a TLS 1.3 handshake under the selected scenario, and records protocol-visible and system-visible metrics. This per-handshake design is intended to preserve the cost of live certificate-based authentication as the basic unit of analysis.

Handshake latency was measured using a monotonic clock source, thereby avoiding wall-clock artifacts and preserving a stable basis for repeated comparisons. At the transport level, the client recorded the number of bytes read and written during the handshake. At the certificate-path level, it recorded the observed chain length and the observed chain size in DER bytes, using the peer certificate chain exposed by the TLS stack together with certificate serialization. A defensive fallback to the leaf certificate was maintained so that the measurement pipeline remained robust even when chain exposure did not match a naive logical expectation.

In addition to protocol-level metrics, the experiments collected performance-counter data on both client and server. These counters were normalized per run in order to support client/server decomposition at the handshake level. The principal performance-counter variables used in the paper are task-clock, instructions, cycles, and derived ratios such as task-clock over elapsed time and server/client task-clock ratio. These variables are not treated as a substitute for full function tracing; their role is to reveal whether a given regime remains balanced, becomes validation-skewed, or becomes overwhelmingly server-bound.

The final execution policy used non-uniform sample sizes across scenarios. Fast scenarios were executed with larger sample counts, whereas extremely heavy scenarios, especially those involving SLH-DSA in the leaf, were run with smaller but still analytically sufficient sample counts. This was a deliberate methodological decision. Since the main structural findings of the paper rest on bounded versus orders-of-magnitude regime differences rather than on tiny marginal effects, the use of non-uniform samples does not undermine the causal interpretation sought here.

5.5 Experimental campaigns

The experimental design is organized into four campaigns, each intended to isolate a distinct question in post-quantum TLS authentication.

Campaign A isolates the leaf effect. It compares scenarios in which the principal change is the signature family used in the server leaf, while keeping the surrounding hierarchy as simple and controlled as possible. Its purpose is to test whether the main discontinuity already appears in the most direct certificate-authentication comparison.

Campaign B studies the full hierarchy strategy space under a common hybrid key-establishment regime. This is the central strategy matrix of the paper. It evaluates complete hierarchy constructions rather than local pairwise substitutions, thereby allowing the study to compare operationally plausible and operationally implausible migration strategies as such.

Campaign C isolates topology from placement by comparing depth 2 and depth 3 hierarchies across comparable algorithmic families. Its purpose is to determine whether increasing chain depth behaves as a simple monotonic penalty or whether the effect depends on which certificates become visible in the effective chain transmitted during the handshake.

Campaign D explores key-establishment variation under comparable chain constructions. It contrasts classical, hybrid, and pure post-quantum KEX modes in order to determine whether the main placement-driven interpretation survives across different key-establishment assumptions.

Taken together, these campaigns define a cumulative analytical structure. Campaign A establishes whether leaf placement alone can trigger the heavy regime. Campaign B identifies the main strategic landscape. Campaign C distinguishes topological effects from placement effects. Campaign D tests whether KEX choice materially alters the dominant hierarchy-sensitive interpretation.

5.6 Metric semantics and normalization

The paper uses a layered metric model. At the handshake level, the main latency variables are `elapsed_mean_ms` and `elapsed_p95_ms`, which capture average and high-percentile latency, respectively. These are the principal observables used to assess interactive plausibility from the perspective of live TLS authentication.

At the transport and chain level, the main variables are `bytes_read_mean`, `bytes_written_mean`, `chain_bytes_unique`, and `served_chain_der_bytes`. The first two track the protocol-visible byte cost of the handshake. The latter two characterize certificate material exposure more directly, although, as discussed below, their semantics are not perfectly homogeneous across all topology classes.

At the performance-counter level, the main variables are `client_task_clock_per_run_ms`, `server_task_clock_per_run_ms`, `instructions`, `cycles`, `IPC`, and derived normalized ratios. These variables make it possible to distinguish among balanced low-cost regimes, client-skewed validation regimes, and overwhelmingly server-bound regimes.

Several metrics are also expressed relative to a common baseline. The baseline scenario used throughout the paper is the hybrid depth 3 fully-ML hierarchy:

```
x25519mlkem768_ml_root_ml_int_ml_leaf.
```

Relative metrics such as latency multiplier, bytes-read multiplier, retained capacity, and server-side compute multiplier are used to make structural contrasts easier to interpret than raw absolute values alone. This normalization is especially important because the experimental space contains both sub-millisecond and second-scale regimes.

Finally, the paper derives capacity and economic interpretations from normalized server-side compute measurements. These derived quantities are not treated as direct billing observations, but as operational translations of per-handshake server burden. Their role is not to produce universal cost prophecy, but to clarify the deployment meaning of the measured authentication regimes.

5.7 Methodological cautions

Several methodological cautions are necessary for correct interpretation of the dataset.

First, the analytical dataset used for cross-cutting interpretation is deduplicated by `scenario_id`. This is necessary because Campaign C intentionally reuses scenarios that also appear in Campaign B. These repeated scenarios were checked for metric consistency and treated as analytical reuse rather than as independent new observations. Campaign identity is preserved where narratively relevant, but scenario-level cross-cutting analysis operates on the deduplicated space.

Second, the observed value `chain_len_unique = 2` does not imply that the logical certification hierarchy has depth 2. In the dataset studied here, the client consistently observes two certificates in the effective chain, but those two certificates do not always correspond to the same logical pair. In

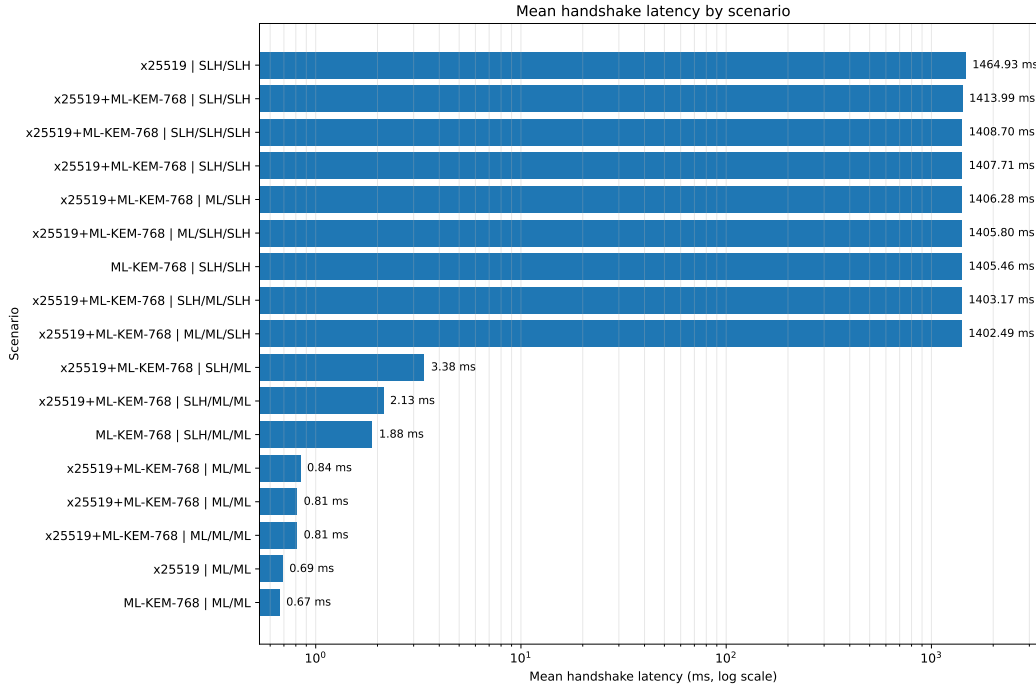


Figure 1: Mean handshake latency by scenario.

depth 2 scenarios, the observed pair may correspond to root plus leaf; in depth 3 scenarios, it may instead correspond to intermediate plus leaf. For that reason, effective chain exposure must be treated as an empirical variable rather than inferred mechanically from declared hierarchy depth.

Third, `served_chain_der_bytes` does not carry identical semantics across all topology classes. In the present dataset, it aligns with leaf DER size in some depth 2 scenarios, whereas in depth 3 scenarios it more closely tracks the observed effective chain. For strict transport reasoning across depths, the more robust observables are therefore `bytes_read_mean` and `chain_bytes_unique`.

Fourth, the performance-counter analysis is intentionally regime-oriented. The paper uses performance-derived data to identify where active work concentrates during the handshake, not to claim complete code-path attribution. Strong claims are therefore made at the level of cost concentration and regime structure rather than at the level of unique internal implementation causes.

These cautions do not weaken the study. On the contrary, they sharpen its interpretive discipline by ensuring that hierarchy, chain exposure, and client/server cost are treated as measured properties of live TLS authentication rather than as naive consequences of abstract scenario labels.

6 Results

6.1 Global performance landscape

The global results do not form a smooth continuum of gradually increasing cost. Instead, the scenario space separates into clearly differentiated operational regimes. At one end, all-ML scenarios remain in a narrow low-latency band below one millisecond. At the other, scenarios with SLH-DSA in the server leaf cluster around a distinct plateau near 1.4 seconds. Between those regions lies a smaller intermediate band, populated mainly by configurations that place SLH-DSA in upper hierarchy layers while preserving ML-DSA in the interactive leaf.

As shown in Figure 1, mean latency spans from approximately 0.665 ms to 1464.933 ms. This is not a modest gradient of penalties, but a separation of regimes. The low-cost region is populated by

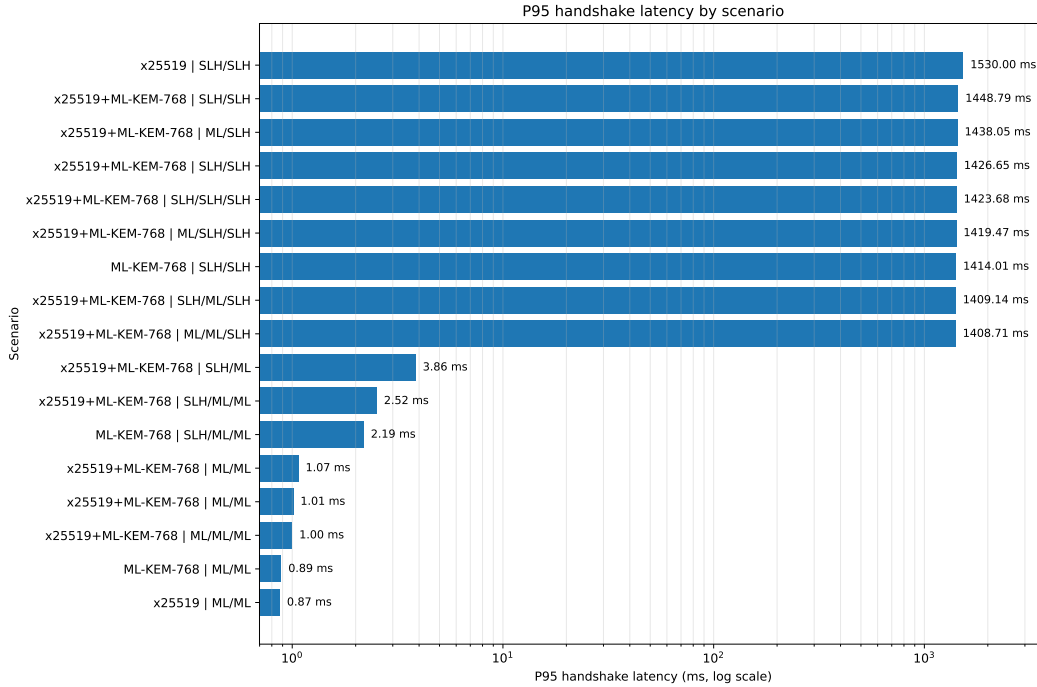


Figure 2: P95 handshake latency by scenario.

Table 1: Master scenario summary (short version).

scenario_id	kex_mode	depth	hierarchy	mean_ms	p95_ms	bytes_read	server_task_ms	srv_cli_ratio
x25519__leaf_mlds65	classical	2	ML root / ML leaf	0.688	0.874	14904	0.529	1.022
x25519__leaf_slhdsashake192s	classical	2	SLH root / SLH leaf	1464.933	1529.999	49881	1462.281	462.869
x25519mlkem768__leaf_mlds65	hybrid	2	ML root / ML leaf	0.841	1.072	15992	0.623	1.049
x25519mlkem768__leaf_slhdsashake192s	hybrid	2	SLH root / SLH leaf	1413.991	1448.787	50969	1411.345	448.264
x25519mlkem768__ml_root_ml_leaf	hybrid	2	ML root / ML leaf	0.809	1.013	15992	0.602	1.044
x25519mlkem768__ml_root_slh_leaf	hybrid	2	SLH root / SLH leaf	1406.283	1438.054	26999	1404.927	696.186
x25519mlkem768__slh_root_ml_leaf	hybrid	2	SLH root / ML leaf	3.376	3.856	39962	1.915	0.998
x25519mlkem768__slh_root_slh_leaf	hybrid	2	SLH root / SLH leaf	1407.714	1426.652	50969	1405.087	441.560
x25519mlkem768__ml_root_ml_int_ml_leaf	hybrid	3	ML root / ML int / ML leaf	0.809	1.000	16008	0.562	0.903
x25519mlkem768__ml_root_ml_int_slh_leaf	hybrid	3	ML root / ML int / SLH leaf	1402.486	1408.711	27015	1401.169	687.949
x25519mlkem768__ml_root_slh_int_slh_leaf	hybrid	3	ML root / SLH int / SLH leaf	1405.803	1419.470	38046	1403.109	433.616
x25519mlkem768__slh_root_ml_int_ml_leaf	hybrid	3	SLH root / ML int / ML leaf	2.133	2.522	28947	0.667	0.346
x25519mlkem768__slh_root_ml_int_slh_leaf	hybrid	3	SLH root / ML int / SLH leaf	1403.166	1409.142	39954	1401.849	430.764
x25519mlkem768__slh_root_slh_int_slh_leaf	hybrid	3	SLH root / SLH int / SLH leaf	1408.703	1423.678	50985	1404.903	326.456
mlkem768__ml_root_ml_leaf	pure_pqc	2	ML root / ML leaf	0.665	0.887	15960	0.515	1.003
mlkem768__slh_root_slh_leaf	pure_pqc	2	SLH root / SLH leaf	1405.456	1414.012	50937	1402.896	463.910
mlkem768__slh_root_ml_int_ml_leaf	pure_pqc	3	SLH root / ML int / ML leaf	1.884	2.186	28915	0.527	0.298

all-ML scenarios together with a limited number of root-SLH / leaf-ML cases. The heavy region is dominated by configurations in which SLH-DSA reaches the leaf.

Figure 2 shows that the same structure persists in high-percentile behavior. The heavy scenarios do not merely shift upward in mean latency; they remain heavy in the upper tail as well. This is operationally important because it shows that the severe regime is not a minor average-case distortion, but a persistent property of the handshake.

A further point is already visible at this stage. The heavy scenarios do not form a broad gradient in which progressively larger chains produce progressively worse latency. Once SLH-DSA is placed in the leaf, they cluster instead into a relatively tight plateau. This already suggests that the main discontinuity is placement-defined rather than the result of incremental transport growth alone.

6.2 Campaign A: leaf-only comparison

Campaign A provides the cleanest entry point into the problem. It isolates the leaf effect while keeping the surrounding hierarchy deliberately simple. It therefore offers the strongest setting in

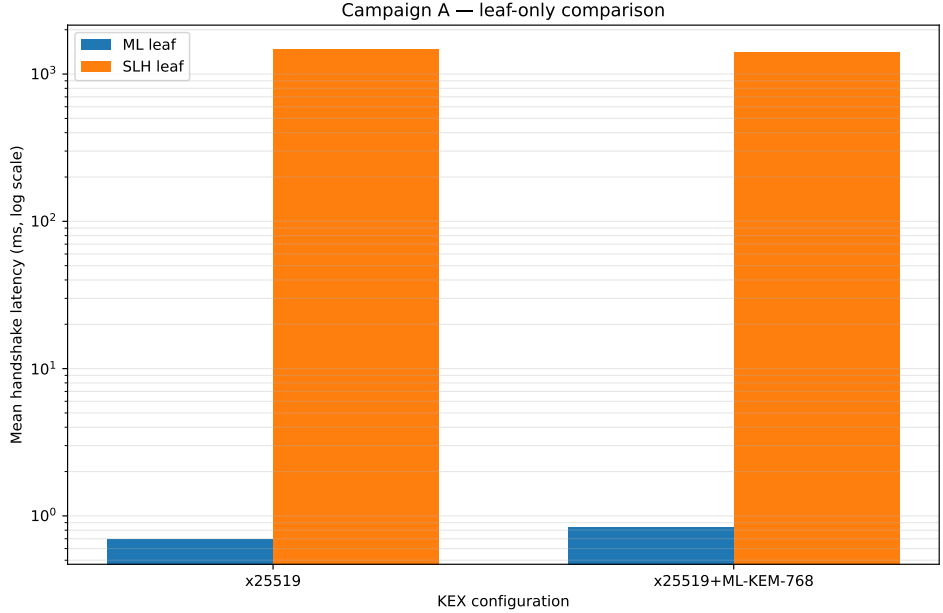


Figure 3: Campaign A: leaf-only comparison.

Table 2: Campaign A paired comparison.

kex_mode	tls_group_family	ml elapsed mean (ms)	slh elapsed mean (ms)	latency ratio SLH / ML	ml bytes read mean	slh bytes read mean	bytes-read ratio SLH / ML
classical	x25519	0.688	1464.933	2127.865	14904	49881	3.347
hybrid	x25519mlkem768	0.841	1413.991	1682.137	15992	50969	3.187

kex_mode	tls_group_family	ml server task clock per run (ms)	slh server task clock per run (ms)	server taskclock ratio SLH / ML	ml client task clock per run (ms)	slh client task clock per run (ms)	client taskclock ratio SLH / ML
classical	x25519	0.529	1462.281	2765.628	0.517	3.159	6.107
hybrid	x25519mlkem768	0.623	1411.345	2265.961	0.594	3.148	5.303

which to test whether the main discontinuity appears as soon as SLH-DSA is introduced into the interactive server leaf.

6.2.1 Classical KEX

Under classical X25519, replacing an ML-DSA leaf with an SLH-DSA leaf produces an extreme discontinuity. Mean latency increases by approximately 2127.86 \times , and p95 by approximately 1750.57 \times . By contrast, the transport expansion is much smaller: bytes_read_mean grows by about 3.35 \times , and chain_bytes_unique by about 2.98 \times .

The same asymmetry appears in the performance counters. Server task-clock per run grows by approximately 2765.63 \times , whereas client task-clock per run grows by only 6.11 \times . Even in this simplest leaf-only configuration, the observed latency jump is therefore far larger than the increase in transmitted certificate material.

6.2.2 Hybrid KEX

The same comparison under hybrid X25519MLKEM768 yields the same qualitative result. Mean latency increases by approximately 1682.14 \times , while p95 rises by approximately 1351.48 \times . Transport growth again remains comparatively modest: bytes_read_mean grows by about 3.19 \times , and chain_bytes_unique by about 2.98 \times .

The performance counters remain consistent with the same interpretation. Server task-clock per run increases by approximately 2265.96 \times , while client task-clock per run increases by only 5.30 \times .

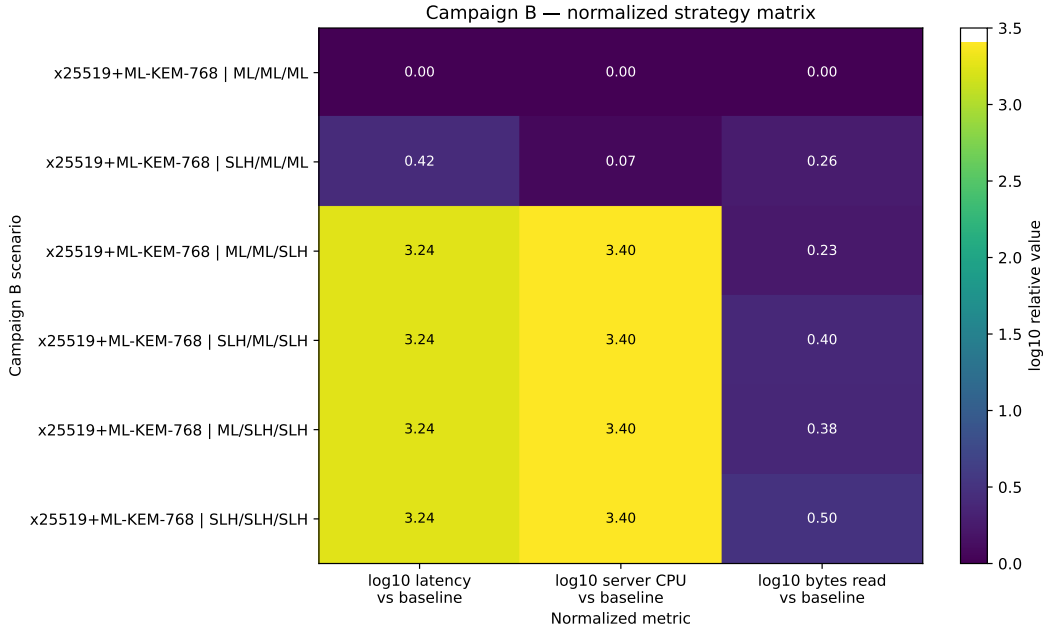


Figure 4: Campaign B: normalized strategy matrix.

Table 3: Campaign B strategy matrix.

scenario_id	slh_position_class	elapsed_mean_ms	bytes_read_mean	server_task_clock_per_run_ms	latency_relative_to_baseline
x25519mlkem768__ml_root_ml_int_ml_leaf	no_slh	0.809000	16008	0.562000	1.000000
x25519mlkem768__slh_root_ml_int_ml_leaf	root	2.133000	28947	0.667000	2.640000
x25519mlkem768__ml_root_ml_int_slh_leaf	leaf	1402.486000	27015	1401.169000	1733.490000
x25519mlkem768__slh_root_ml_int_slh_leaf	root_and_leaf	1403.166000	39954	1401.849000	1734.330000
x25519mlkem768__ml_root_slh_int_slh_leaf	intermediate_and_leaf	1405.803000	38046	1403.109000	1737.590000
x25519mlkem768__slh_root_slh_int_slh_leaf	root_and_intermediate_and_leaf	1408.703000	50985	1404.903000	1741.180000

scenario_id	slh_position_class	server_cpu_relative_to_baseline	bytes_read_relative_to_baseline	operational_plausibility
x25519mlkem768__ml_root_ml_int_ml_leaf	no_slh	1.000000	1.000000	Reasonable
x25519mlkem768__slh_root_ml_int_ml_leaf	root	1.190000	1.810000	Penalized but plausible
x25519mlkem768__ml_root_ml_int_slh_leaf	leaf	2493.640000	1.690000	Unsuitable for interactive TLS front-end
x25519mlkem768__slh_root_ml_int_slh_leaf	root_and_leaf	2494.850000	2.500000	Unsuitable for interactive TLS front-end
x25519mlkem768__ml_root_slh_int_slh_leaf	intermediate_and_leaf	2497.090000	2.380000	Unsuitable for interactive TLS front-end
x25519mlkem768__slh_root_slh_int_slh_leaf	root_and_intermediate_and_leaf	2500.280000	3.180000	Unsuitable for interactive TLS front-end

The heavy regime is therefore already visible in the simplest leaf-only comparison and cannot be dismissed as a by-product of deeper hierarchies or more elaborate mixed chains.

6.2.3 Main result of Campaign A

Campaign A establishes the first decisive empirical result of the paper: the dominant operational collapse does not require a complex hierarchy, a mixed certification strategy, or a pure post-quantum key-establishment path. It already appears when SLH-DSA is moved into the server leaf certificate. In other words, the main discontinuity is visible before the analysis reaches the full hierarchy design space.

6.3 Campaign B: full hierarchy strategy matrix

Campaign B is the central strategic core of the study. Unlike Campaign A, which isolates a single placement change, Campaign B evaluates full hierarchy constructions under a common hybrid key-establishment regime. This makes it possible to compare migration strategies as complete authentication designs rather than as local substitutions.

Table 4: Campaign B operational plausibility ranking.

plausibility_rank	scenario_id	hierarchy_family_label	slh_position_class	elapsed_mean_ms	server_task_clock_per_run_ms	operational_plausibility
1	x25519mlkem768_ml_root_ml_int_ml_leaf	ML root / ML int / ML leaf	no_slh	0.809000	0.562000	Reasonable
2	x25519mlkem768_slh_root_ml_int_ml_leaf	SLH root / ML int / ML leaf	root	2.133000	0.667000	Penalized but plausible
4	x25519mlkem768_ml_root_ml_int_slh_leaf	ML root / ML int / SLH leaf	leaf	1402.486000	1401.169000	Unsuitable for interactive TLS front-end
4	x25519mlkem768_slh_root_ml_int_slh_leaf	SLH root / ML int / SLH leaf	root_and_leaf	1403.166000	1401.849000	Unsuitable for interactive TLS front-end
4	x25519mlkem768_ml_root_slh_int_slh_leaf	ML root / SLH int / SLH leaf	intermediate_and_leaf	1405.803000	1403.109000	Unsuitable for interactive TLS front-end
4	x25519mlkem768_slh_root_slh_int_slh_leaf	SLH root / SLH int / SLH leaf	root_and_intermediate_and_leaf	1408.703000	1404.903000	Unsuitable for interactive TLS front-end

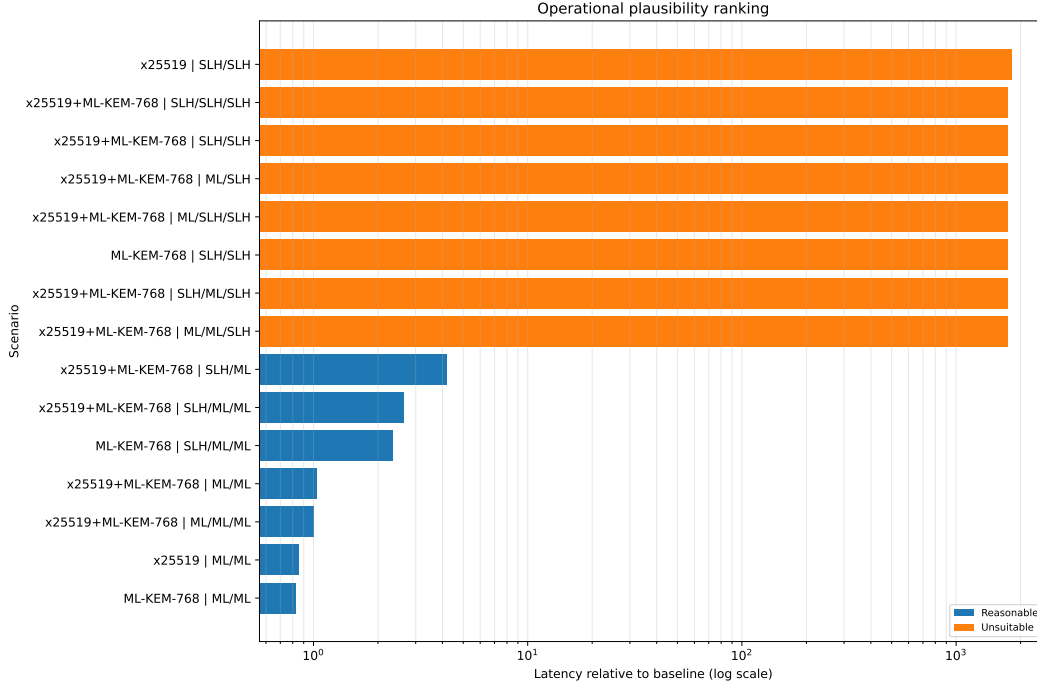


Figure 5: Operational plausibility ranking by scenario, expressed as latency relative to the fully-ML baseline.

6.3.1 Fully-ML baseline

The baseline strategy for Campaign B is the hybrid depth-3 hierarchy `x25519mlkem768_ml_root_ml_int_ml_leaf`. Its mean latency is 0.809 ms, its p95 is 1.000 ms, it reads 16008 bytes per handshake on average, and its server task-clock per run is approximately 0.562 ms. This configuration serves as the reference point for the relative comparisons reported throughout the paper.

6.3.2 Root-SLH with ML leaf

The most important bounded-penalty case in Campaign B is `x25519mlkem768_slh_root_ml_int_ml_leaf`. Relative to the fully-ML baseline, its mean latency rises by approximately $2.64\times$, its server task-clock increases by only about $1.19\times$, and its read volume increases by about $1.81\times$. This is a real penalty, but not a collapse. The scenario remains within an interactive regime and stands out as the only non-baseline strategy in Campaign B that survives a strict operational reading.

6.3.3 Leaf-SLH strategies

The remaining mixed strategies in Campaign B all place SLH-DSA in the leaf. Once that happens, the design space collapses into a narrow catastrophic band. Mean latency ranges from approximately 1402.486 ms to 1408.703 ms, corresponding to roughly $1733.49\times$ to $1741.18\times$ the fully-ML baseline. At the same time, server task-clock grows by approximately $2493.64\times$ to $2500.28\times$, while read volume grows by only about $1.69\times$ to $3.18\times$.

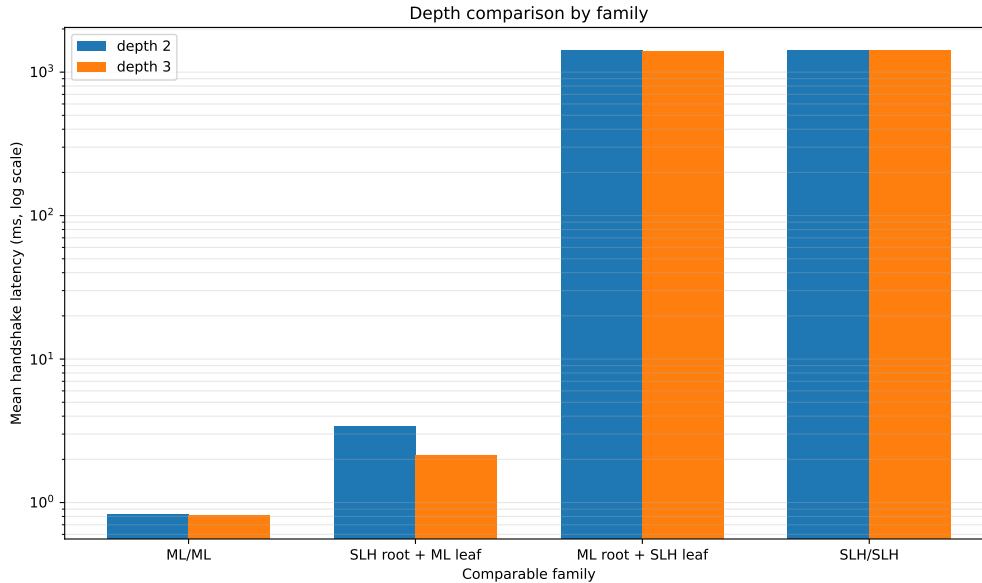


Figure 6: Depth comparison by family.

This concentration is itself informative. Once SLH-DSA reaches the leaf, mixed hierarchy details cease to explain much of the observed latency spread. The main explanatory break is therefore not between one mixed hierarchy and another, but between non-leaf-SLH and leaf-SLH configurations.

6.3.4 Main result of Campaign B

Campaign B is where the strategic thesis of the paper becomes fully visible. The variable with the greatest explanatory power is not whether SLH-DSA appears somewhere in the hierarchy, but whether it appears in the leaf exposed to the live TLS handshake. Figure 5 shows this compactly: the fully-ML baseline remains in the reasonable region, the root SLH / intermediate ML / leaf ML strategy remains penalized but plausible, and the moment SLH-DSA reaches the leaf the remaining strategies move into the operationally unsuitable region.

6.4 Campaign C: depth comparison

Campaign C separates topology from signature placement. Methodologically, this is one of the most important parts of the study because it shows that increasing hierarchy depth does not behave as a simple monotonic penalty. The cost effect of moving from depth 2 to depth 3 depends on which certificates become part of the effective chain observed during the handshake.

6.4.1 All-ML families

In the fully-ML family, depth does not introduce a meaningful penalty. Comparing `x25519mlkem768__ml_root__ml_leaf` with `x25519mlkem768__ml_root__ml_int__ml_leaf`, the latency ratio is effectively 1.00, with only negligible differences in observed bytes and a slightly smaller server task-clock in the depth-3 case. Depth alone is therefore not sufficient to degrade a well-behaved ML hierarchy in any meaningful way.

6.4.2 Root-SLH with ML leaf

The clearest topological effect appears when the root uses SLH-DSA while the leaf remains ML-DSA. In that family, the depth-3 variant is substantially cheaper than the depth-2 one. The latency ratio falls to approximately 0.6318, corresponding to a reduction of about 36.8% in mean latency. At the same time, `bytes_read_mean` decreases by about 11015 bytes and `chain_bytes_unique` by about 10993 bytes.

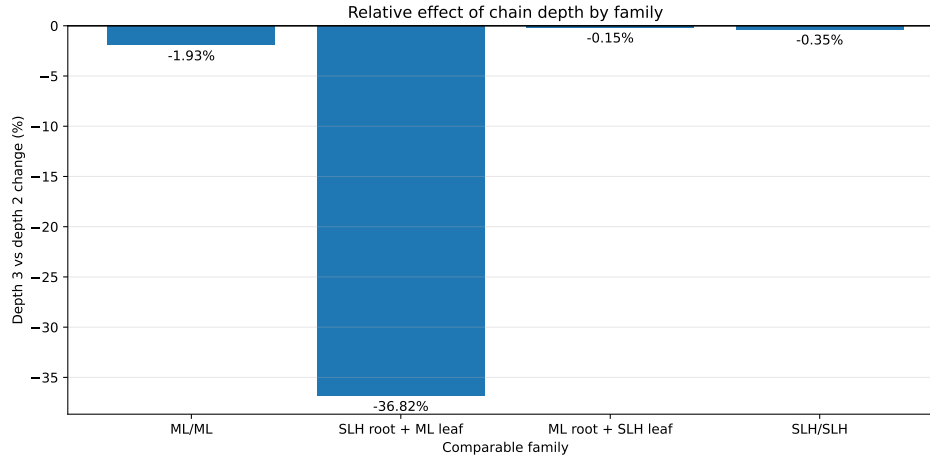


Figure 7: Relative effect of moving from depth 2 to depth 3 by comparable family, expressed as percentage change in mean latency.

Table 5: Depth 2 vs. depth 3 comparisons.

pair label	depth 2 scenario_id	depth 3 scenario_id	depth 2 elapsed mean (ms)	depth 3 elapsed mean (ms)	delta elapsed mean (ms) d3 minus d2	latency ratio d3 / d2
ML/ML	x25519mlkem768__ml_ro ot__ml_leaf	x25519mlkem768__ml_root_ _ml_int__ml_leaf	0.809300	0.809100	-0.000200	0.999700
SLH root + ML leaf	x25519mlkem768__slh_ro ot__ml_leaf	x25519mlkem768__slh_root_ _ml_int__ml_leaf	3.376200	2.133000	-1.243100	0.631800
ML root + SLH leaf (ML intermediate)	x25519mlkem768__ml_ro ot__slh_leaf	x25519mlkem768__ml_root_ _ml_int__slh_leaf	1406.283200	1402.486200	-3.797000	0.997300
ML root + SLH leaf (SLH intermediate)	x25519mlkem768__ml_ro ot__slh_leaf	x25519mlkem768__ml_root_ _slh_int__slh_leaf	1406.283200	1405.802800	-0.480400	0.999700
SLH/SLH (ML intermediate)	x25519mlkem768__slh_ro ot__slh_leaf	x25519mlkem768__slh_root_ _ml_int__slh_leaf	1407.714100	1403.165900	-4.548200	0.996800
SLH/SLH (SLH intermediate)	x25519mlkem768__slh_ro ot__slh_leaf	x25519mlkem768__slh_root_ _slh_int__slh_leaf	1407.714100	1408.703300	0.989200	1.000700

pair label	depth 2 scenario_id	depth 3 scenario_id	delta bytes read mean d3 minus d2	delta chain bytes unique d3 minus d2	delta server task clock per run (ms) d3 minus d2	server taskclock ratio d3 / d2
ML/ML	x25519mlkem768__ml_ro ot__ml_leaf	x25519mlkem768__ml_root_ _ml_int__ml_leaf	16	16	-0.040300	0.933100
SLH root + ML leaf	x25519mlkem768__slh_ro ot__ml_leaf	x25519mlkem768__slh_root_ _ml_int__ml_leaf	-11015	-10993	-1.247500	0.348500
ML root + SLH leaf (ML intermediate)	x25519mlkem768__ml_ro ot__slh_leaf	x25519mlkem768__ml_root_ _ml_int__slh_leaf	16	16	-3.757500	0.997300
ML root + SLH leaf (SLH intermediate)	x25519mlkem768__ml_ro ot__slh_leaf	x25519mlkem768__ml_root_ _slh_int__slh_leaf	11047	11025	-1.817400	0.998700
SLH/SLH (ML intermediate)	x25519mlkem768__slh_ro ot__slh_leaf	x25519mlkem768__slh_root_ _ml_int__slh_leaf	-11015	-10993	-3.238100	0.997700
SLH/SLH (SLH intermediate)	x25519mlkem768__slh_ro ot__slh_leaf	x25519mlkem768__slh_root_ _slh_int__slh_leaf	16	16	-0.183900	0.999900

The interpretation follows from effective chain exposure. In the depth-2 variant, the observed chain corresponds to root plus leaf; in the depth-3 variant, it corresponds to intermediate plus leaf. Since the root is the heavy SLH signer in this family, removing it from the observed chain materially reduces visible transport and overall cost.

6.4.3 Leaf-SLH families

The leaf-SLH families show the opposite pattern. Once SLH-DSA reaches the leaf, changes in depth still affect transport, sometimes substantially, but they have little effect on latency. In the ML root + SLH leaf family, the depth ratio remains effectively 1.00 even when one depth-3 variant increases observed transport by more than 11 KB. In the SLH/SLH family, depth may either reduce or increase observed transport, yet latency remains nearly unchanged.

This is one of the clearest indications that depth continues to matter for transport while ceasing to govern the main latency regime once the leaf itself becomes the dominant source of cryptographic cost.

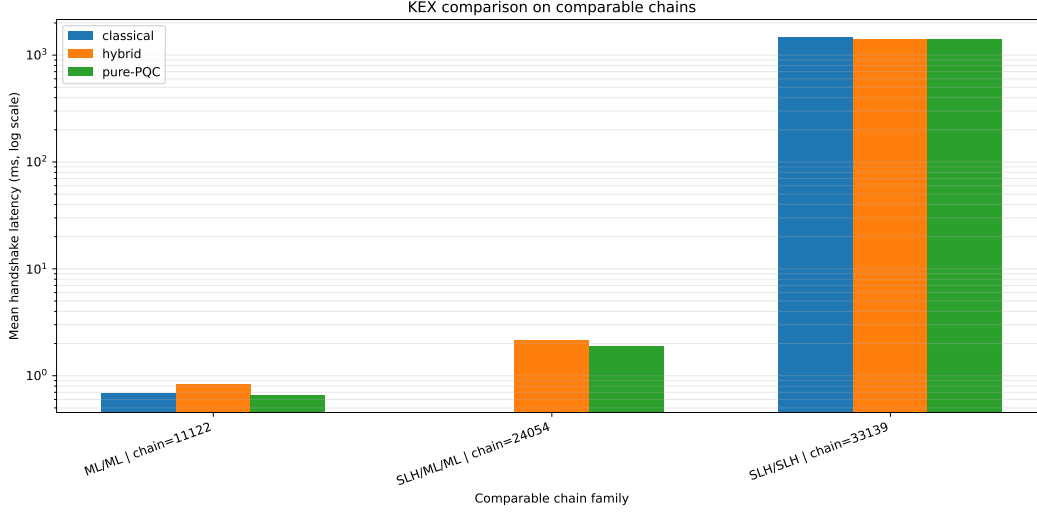


Figure 8: KEX comparison on comparable chains.

Table 6: KEX comparisons on comparable chains.

comparison_type	family_label	from_kex_mode	to_kex_mode	leaf_family	depth	elapsed_mean_from_ms	elapsed_mean_to_ms	latency_ratio_to_over_from
classical_vs_hybrid	ML root / ML leaf (depth 2)	classical	hybrid	ML-DSA	2	0.6885	0.8406	1.2210
classical_vs_hybrid	SLH root / SLH leaf (depth 2)	classical	hybrid	SLH-DSA	2	1464.9327	1413.9914	0.9652
hybrid_vs_pure_pqc	ML root / ML leaf (depth 2)	hybrid	pure_pqc	ML-DSA	2	0.8093	0.6652	0.8220
hybrid_vs_pure_pqc	SLH root / ML int / ML leaf (depth 3)	hybrid	pure_pqc	ML-DSA	3	2.1330	1.8842	0.8833
hybrid_vs_pure_pqc	SLH root / SLH leaf (depth 2)	hybrid	pure_pqc	SLH-DSA	2	1407.7141	1405.4559	0.9984

comparison_type	family_label	from_kex_mode	to_kex_mode	leaf_family	depth	bytes_read_from	bytes_read_to	bytes_read_ratio_to_over_from
classical_vs_hybrid	ML root / ML leaf (depth 2)	classical	hybrid	ML-DSA	2	14904	15992	1.0730
classical_vs_hybrid	SLH root / SLH leaf (depth 2)	classical	hybrid	SLH-DSA	2	49881	50969	1.0218
hybrid_vs_pure_pqc	ML root / ML leaf (depth 2)	hybrid	pure_pqc	ML-DSA	2	15992	15960	0.9980
hybrid_vs_pure_pqc	SLH root / ML int / ML leaf (depth 3)	hybrid	pure_pqc	ML-DSA	3	28947	28915	0.9989
hybrid_vs_pure_pqc	SLH root / SLH leaf (depth 2)	hybrid	pure_pqc	SLH-DSA	2	50969	50937	0.9994

comparison_type	family_label	from_kex_mode	to_kex_mode	leaf_family	depth	server_task_from_ms	server_task_to_ms	server_task_ratio_to_over_from
classical_vs_hybrid	ML root / ML leaf (depth 2)	classical	hybrid	ML-DSA	2	0.5287	0.6228	1.1780
classical_vs_hybrid	SLH root / SLH leaf (depth 2)	classical	hybrid	SLH-DSA	2	1462.2813	1411.3448	0.9652
hybrid_vs_pure_pqc	ML root / ML leaf (depth 2)	hybrid	pure_pqc	ML-DSA	2	0.6022	0.5152	0.8555
hybrid_vs_pure_pqc	SLH root / ML int / ML leaf (depth 3)	hybrid	pure_pqc	ML-DSA	3	0.6672	0.5273	0.7903
hybrid_vs_pure_pqc	SLH root / SLH leaf (depth 2)	hybrid	pure_pqc	SLH-DSA	2	1405.0874	1402.8960	0.9984

6.4.4 Main result of Campaign C

Campaign C shows that hierarchy depth is not itself a cost verdict. Whether depth penalizes, preserves, or even reduces observed cost depends on how the topology changes the effective chain seen during the handshake. This point is especially important for the interpretation of post-quantum certificate hierarchies, since it shows that logical depth and practical exposure cannot be treated as interchangeable notions.

6.5 Campaign D: KEX mode exploration

Campaign D serves as a focused validation layer. Its purpose is not to overturn the interpretation established by the earlier campaigns, but to test whether moving from classical to hybrid, or from hybrid to pure post-quantum key establishment, materially changes the placement-driven picture once comparable chains are held fixed.

In ML-leaf regimes, KEX choice does modulate the cost profile. For example, moving from classical to hybrid in the simple ML-leaf case increases latency by about $1.2210\times$, while moving from hybrid to pure post-quantum reduces it to about $0.8220\times$ the hybrid value. Similar but still bounded effects are visible in the SLH root / ML int / ML leaf family, where hybrid to pure post-quantum produces a latency ratio of about $0.8833\times$.

By contrast, once the leaf uses SLH-DSA, KEX mode becomes almost irrelevant to the dominant regime. In the SLH root / SLH leaf comparison, classical to hybrid yields a latency ratio of about

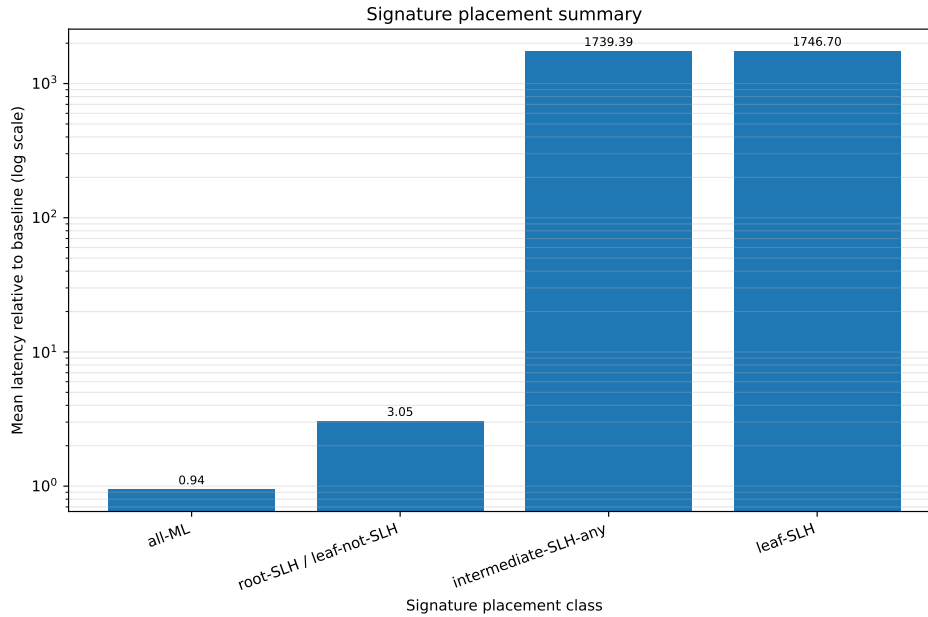


Figure 9: Signature placement summary.

$0.9652\times$, and hybrid to pure post-quantum about $0.9984\times$. These are local perturbations inside an already catastrophic regime.

6.5.1 Main result of Campaign D

Campaign D closes the KEX question cleanly. KEX mode matters in low-cost ML-leaf scenarios and can produce moderate changes in bounded regimes. It does not, however, materially alter the central interpretation of the study. Pure post-quantum key establishment does not reverse the main picture. The decisive variable remains signature placement, and especially the decision to place SLH-DSA in the handshake-exposed server leaf.

7 Cross-Cutting Cryptographic Interpretation

The campaign-based results already establish the main empirical structure of the study. However, their broader significance becomes clearer when the evidence is reorganized around four cross-cutting questions: whether signature placement explains behavior better than signature-family presence alone, whether transport-related overhead is sufficient to explain the heavy regime, whether effective chain exposure must be treated as part of the phenomenon rather than as a secondary implementation artifact, and whether the leaf-SLH cases form a distinct operational regime rather than the upper end of a continuous cost spectrum. Read in that way, the results support a sharper interpretation of post-quantum TLS authentication as a hierarchy-sensitive cryptographic design problem.

7.1 Signature placement versus mere signature presence

The most compact way to state the central empirical finding of the paper is that signature placement explains the observed authentication regimes better than mere signature-family presence. Once the scenarios are grouped by placement class rather than by campaign, the main structure of the data becomes considerably clearer.

Figure 9 and Table 7 organize the scenario space into four categories: all-ML, root-SLH with non-SLH leaf, intermediate-SLH-any, and leaf-SLH. The all-ML class defines the low-cost reference regime of the study. Its mean latency is approximately 0.7625 ms, with mean server-side compute essentially aligned with the baseline. In practical terms, these scenarios form a tight and stable low-cost cluster.

Table 7: Signature placement summary.

placement_class	n_scenarios	mean_elapsed_ms	median_elapsed_ms	min_elapsed_ms	max_elapsed_ms	mean_latency_vs_baseline
all_ml	5	0.763	0.809	0.665	0.841	0.942
root_slh_leaf_not_slh	3	2.464	2.133	1.884	3.376	3.046
intermediate_slh_any	2	1407.253	1407.253	1405.803	1408.703	1739.386
leaf_slh	9	1413.171	1406.283	1402.486	1464.933	1746.701

placement_class	median_latency_vs_baseline	mean_bytes_vs_baseline	mean_server_cpu_vs_baseline	mean_server_over_elapsed	mean_client_over_elapsed
all_ml	1.000	0.985	1.008	0.744	0.742
root_slh_leaf_not_slh	2.636	2.037	1.844	0.387	0.803
intermediate_slh_any	1739.386	2.781	2498.686	0.998	0.003
leaf_slh	1738.188	2.678	2510.849	0.998	0.002

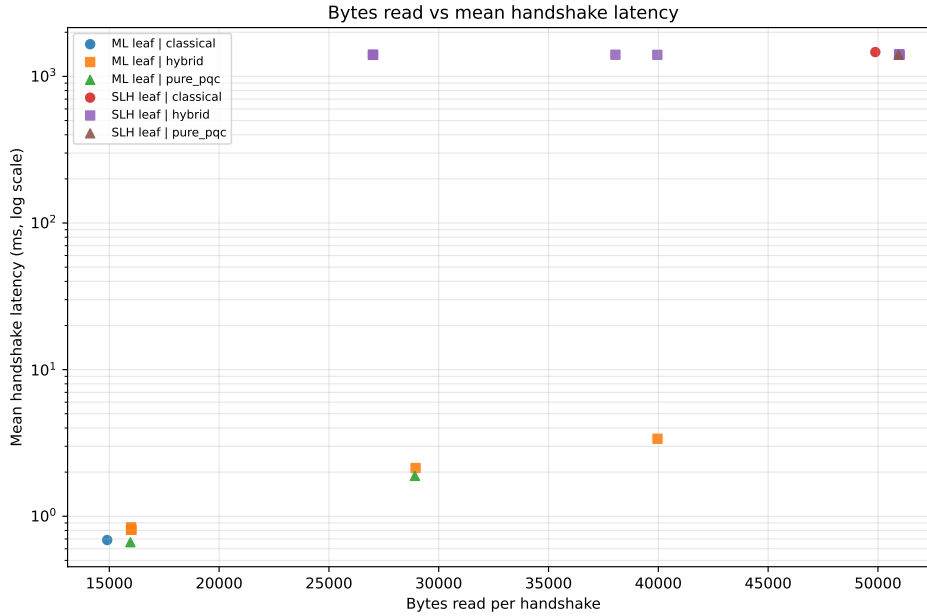


Figure 10: Bytes read versus mean handshake latency.

The `root-SLH / leaf-not-SLH` class is clearly more expensive than all-ML, but it remains within a bounded interactive regime. Its mean latency rises to approximately 2.4645 ms, corresponding to a mean multiplier of about $3.0461 \times$ relative to baseline, while server-side compute rises by about $1.8444 \times$. This is a genuine penalty, but not a regime collapse. The presence of SLH-DSA in the hierarchy is therefore not, by itself, enough to force the handshake into the catastrophic region.

By contrast, the `leaf-SLH` class defines the heavy regime of the study. Its mean latency reaches approximately 1413.1706 ms, with a mean latency multiplier of approximately $1746.7007 \times$ relative to baseline and a mean server-side compute multiplier of approximately $2510.8488 \times$. The contrast is too strong to be read as a mere extension of the upper-layer SLH penalty. Moving from all-ML to upper-layer SLH produces a bounded increase. Moving from upper-layer SLH to leaf-SLH produces a discontinuity.

This distinction is the strongest expression of the paper’s main thesis. The decisive variable is not whether SLH-DSA appears somewhere in the certification path, but whether it crosses into the handshake-exposed leaf. In that sense, hierarchy position has greater explanatory force than signature-family presence taken in the abstract.

7.2 Transport-related overhead versus cryptographic cost

A tempting simplification in post-quantum TLS evaluation is to treat certificate overhead primarily as a wire-cost problem. The data support a more qualified interpretation. Transport-related overhead is relevant and, outside the heavy regime, often highly informative. It is not, however, sufficient to explain the catastrophic behavior associated with leaf-SLH scenarios.

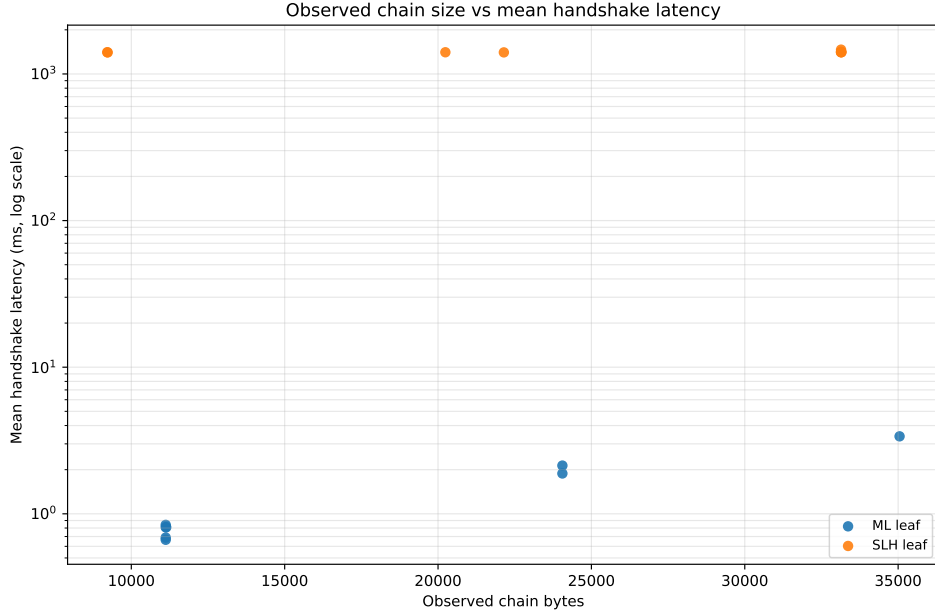


Figure 11: Observed chain size versus mean handshake latency.

Table 8: Transport-versus-latency correlations.

subset	n_scenarios	metric	pearson_r	spearman_rho
all_scenarios	17	bytes_read_mean	0.7493	0.8503
all_scenarios	17	chain_bytes_unique	0.3943	0.5227
non_leaf_slh	8	bytes_read_mean	0.9937	0.8982
non_leaf_slh	8	chain_bytes_unique	0.9933	0.8045
leaf_slh_only	9	bytes_read_mean	0.3518	0.5523
leaf_slh_only	9	chain_bytes_unique	0.3826	0.5919

Over the full dataset, latency exhibits a moderate positive relationship with `bytes_read_mean` and a weaker one with `chain_bytes_unique`. At first glance, this might suggest that the heavy scenarios are simply the outcome of larger transmitted objects. But once leaf-SLH scenarios are excluded, the transport signal becomes much sharper: in the non-catastrophic region, latency tracks both `bytes_read_mean` and `chain_bytes_unique` extremely closely. In other words, transport does explain a great deal while the system remains in a bounded regime.

The picture changes once the analysis is restricted to the leaf-SLH cases. Within that region, the relation between latency and transport weakens sharply. Very large latency persists despite only moderate variation in transferred bytes and observed chain size. Figures 10 and 11 make this visible geometrically: outside leaf-SLH, the points follow a relatively coherent growth pattern; inside leaf-SLH, they collapse into a heavy cloud whose internal latency variation is poorly explained by transport.

The counterexamples in Table 9 are especially revealing. A scenario may transmit more bytes and still remain hundreds of times faster than another scenario that transmits fewer bytes, provided the former keeps SLH-DSA out of the leaf while the latter places it directly in the interactive certificate. That pattern cannot be reduced to wire expansion alone.

The correct interpretation is therefore layered. Transport overhead is real and remains highly relevant in bounded regimes. It is not the dominant explanatory variable once SLH-DSA reaches the leaf. At that point, the main cost source is no longer best described as certificate size or transmitted bytes, but as concentrated cryptographic work during live authentication.

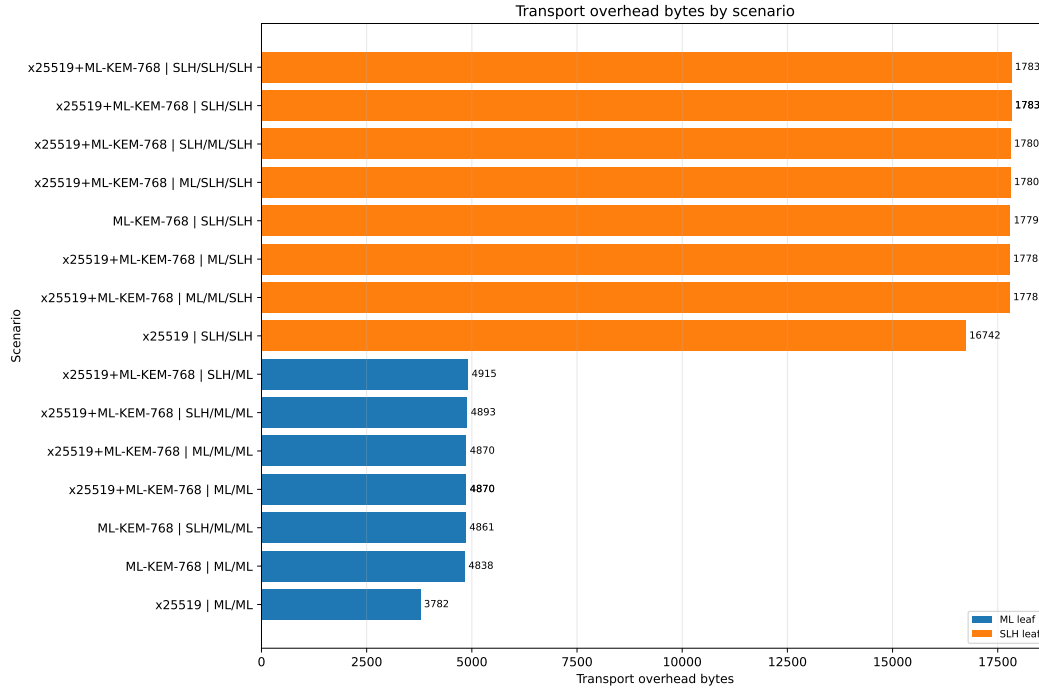


Figure 12: Transport overhead bytes by scenario.

Table 9: Counterexamples to wire-size-only explanations.

rank	transport metric	scenario more bytes lower latency	scenario less bytes higher latency	more bytes value	less bytes value	bytes diff	lower latency (ms)	higher latency (ms)	latency ratio higher / lower
1	bytes_read_mean	x25519mlkem768_slh_root_ml_leaf	x25519mlkem768_ml_root_slh_leaf	39962.0000	26999.0000	12963.0000	3.3762	1406.2832	416.5316
2	bytes_read_mean	x25519mlkem768_slh_root_ml_leaf	x25519mlkem768_ml_root_ml_int_slh_leaf	39962.0000	27015.0000	12947.0000	3.3762	1402.4862	415.4070
3	bytes_read_mean	mlkem768_slh_root_ml_int_ml_leaf	x25519mlkem768_ml_root_slh_leaf	28915.0000	26999.0000	1916.0000	1.8842	1406.2832	746.3713
4	bytes_read_mean	x25519mlkem768_slh_root_ml_int_ml_leaf	x25519mlkem768_ml_root_slh_leaf	28947.0000	26999.0000	1948.0000	2.1330	1406.2832	659.2901
5	bytes_read_mean	mlkem768_slh_root_ml_int_ml_leaf	x25519mlkem768_ml_root_ml_int_slh_leaf	28915.0000	27015.0000	1900.0000	1.8842	1402.4862	744.3561

rank	transport metric	scenario more bytes lower latency	scenario less bytes higher latency	more bytes value	less bytes value	bytes diff	lower latency (ms)	higher latency (ms)	latency ratio higher / lower
1	chain_bytes_unique	x25519mlkem768_slh_root_ml_leaf	x25519mlkem768_ml_root_slh_leaf	35047.0000	9214.0000	25833.0000	3.3762	1406.2832	416.5316
2	chain_bytes_unique	x25519mlkem768_slh_root_ml_leaf	x25519mlkem768_ml_root_ml_int_slh_leaf	35047.0000	9230.0000	25817.0000	3.3762	1402.4862	415.4070
3	chain_bytes_unique	mlkem768_slh_root_ml_int_ml_leaf	x25519mlkem768_ml_root_slh_leaf	24054.0000	9214.0000	14840.0000	1.8842	1406.2832	746.3713
4	chain_bytes_unique	mlkem768_slh_root_ml_int_ml_leaf	x25519mlkem768_ml_root_ml_int_slh_leaf	24054.0000	9230.0000	14824.0000	1.8842	1402.4862	744.3561
5	chain_bytes_unique	x25519mlkem768_slh_root_ml_int_ml_leaf	x25519mlkem768_ml_root_slh_leaf	24054.0000	9214.0000	14840.0000	2.1330	1406.2832	659.2901

7.3 Effective chain exposure as a first-class variable

The transport findings become fully intelligible only once effective chain exposure is treated as a first-class analytical variable. The logical PKI hierarchy is not the whole story. What matters for the handshake is the chain that is actually exposed and processed during protocol execution.

Campaign C provides the clearest demonstration of this point. In the root-SLH / leaf-ML family, moving from depth 2 to depth 3 reduces latency substantially rather than increasing it. The reason is not mysterious once effective exposure is measured instead of assumed. In the depth 2 case, the observed chain corresponds to root plus leaf; in the depth 3 case, it corresponds to intermediate plus leaf. Since the root is the heavy SLH signer in that family, removing it from the effective chain materially reduces both visible transport and overall cost.

This result has a broader methodological implication. Effective chain exposure is not a mere representational detail, nor an implementation nuisance to be abstracted away after the fact. It is part of the cryptographic-protocol phenomenon being studied. It determines which certificates are actually transmitted, which signature objects become part of the authenticated path, and which validation burden becomes visible during the handshake.

The point is particularly important in post-quantum settings because certificate families may differ sharply in footprint and processing cost. Under those conditions, the gap between declared hierarchy and effective exposure can become operationally decisive. A study that models only logical hierarchy depth, while ignoring which certificates actually appear in the live chain, risks missing one of the central mechanisms through which authentication cost is shaped.

For that reason, this paper treats effective chain exposure not as a secondary caveat but as one of the main explanatory variables. The distinction between root-plus-leaf and intermediate-plus-leaf is not merely descriptive. It is one of the mechanisms through which hierarchy design changes the cryptographic surface of the TLS handshake.

7.4 Emergence of a distinct leaf-SLH regime

The evidence presented so far supports a stronger claim than the statement that some scenarios are slower than others. It supports the conclusion that the leaf-SLH cases form a distinct operational regime.

This regime is characterized by four simultaneous properties. First, it exhibits a stable latency plateau around 1.4 seconds rather than a broad gradient of increasingly bad cases. Second, it is tightly linked to signature placement: once SLH-DSA reaches the leaf, the heavy regime appears consistently across campaigns, topology variants, and KEX modes. Third, its relation to transport weakens sharply, as shown by the transport correlations and the wire-size counterexamples. Fourth, it is comparatively insensitive to changes in key-establishment mode, as Campaign D shows.

Taken together, these properties indicate that leaf-SLH is not simply the expensive end of an otherwise continuous design space. It is a qualitatively different authentication regime with its own internal regularity. The scenarios in that class do vary in transmitted bytes, chain composition, and hierarchy structure, but they remain confined to a common heavy band whose defining feature is the placement of SLH-DSA in the handshake-exposed leaf.

This is why the paper treats leaf-SLH as a regime concept rather than as a single bad design point. The experimental campaigns do not merely identify one unfortunate configuration. They reveal a recurring structure in which certificate placement drives the handshake into a state that is transport-insufficiently explained, highly stable across scenario variants, and operationally distinct from both the all-ML baseline and the bounded upper-layer-SLH cases.

The next section deepens that interpretation by asking where the cost of this regime actually resides. If leaf-SLH defines a distinct state of TLS authentication, the natural causal question is whether that state is balanced across both peers, validation-skewed, or overwhelmingly concentrated on the server side.

8 Client/Server Cost Decomposition

The previous sections established that leaf-SLH scenarios form a distinct heavy regime and that transport-related overhead alone does not explain their cost. The next step is therefore causal rather than merely descriptive: where does the active cryptographic burden reside during the handshake? Answering that question requires a client/server decomposition of the authentication path.

8.1 Why client-only observations were insufficient

Earlier stages of the TLS benchmarking work already suggested that client-side activity could not account for the second-scale latency observed in the heaviest scenarios. However, client-only observations were necessarily incomplete. They could show that the client was not consuming enough active CPU time to justify the total elapsed duration, but they could not determine where the missing time was actually being spent.

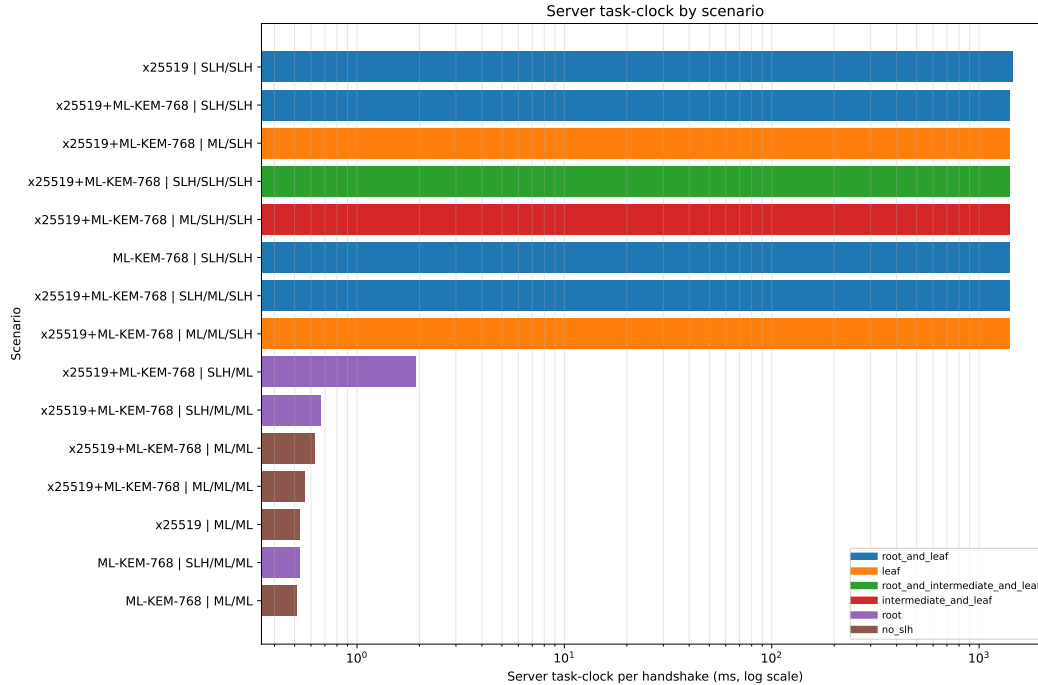


Figure 13: Server task-clock by scenario.

That attribution gap matters. A slow handshake may result from heavier client-side validation, heavier server-side authentication work, roughly symmetric stress on both sides, or waiting behavior dominated by one peer while the other remains active. Without server-side measurements, those possibilities remain partially entangled. The inclusion of server-side performance counters in the final dataset closes that gap and allows the heavy regime to be interpreted in workload terms rather than only in latency terms.

This section therefore asks a narrower causal question than the previous one. Given that leaf-SLH defines a distinct heavy regime, is that regime balanced across client and server, shifted toward validation on the client, or overwhelmingly concentrated on the server side? The answer is one of the central results of the paper.

8.2 Balanced regime in all-ML scenarios

The all-ML class remains the reference regime not only in latency but also in workload structure. Across those scenarios, mean client task-clock is approximately 0.5647 ms, while mean server task-clock is approximately 0.5662 ms. Normalized by elapsed time, the client contributes about 0.7423 of elapsed time in active work and the server about 0.7444. The mean server/client task-clock ratio is approximately 1.0043, and the mean server/client instruction ratio is approximately 1.0841.

These values describe a regime that is not only cheap but also structurally balanced. Both ends of the handshake perform comparable amounts of active work, and neither dominates the other. Figure 14 shows this directly: in the low-cost all-ML region, client and server bars remain of similar magnitude. Figure 15 shows the same structure geometrically, with all-ML scenarios clustering close to the parity line. Figure 17 reinforces the point through ratios close to one.

This balanced structure is important because it provides the control case against which the remaining regimes can be interpreted. Without it, the heavy scenarios might be read merely as more expensive instances of the same general phenomenon. The decomposition shows that they are qualitatively different in where active work resides.

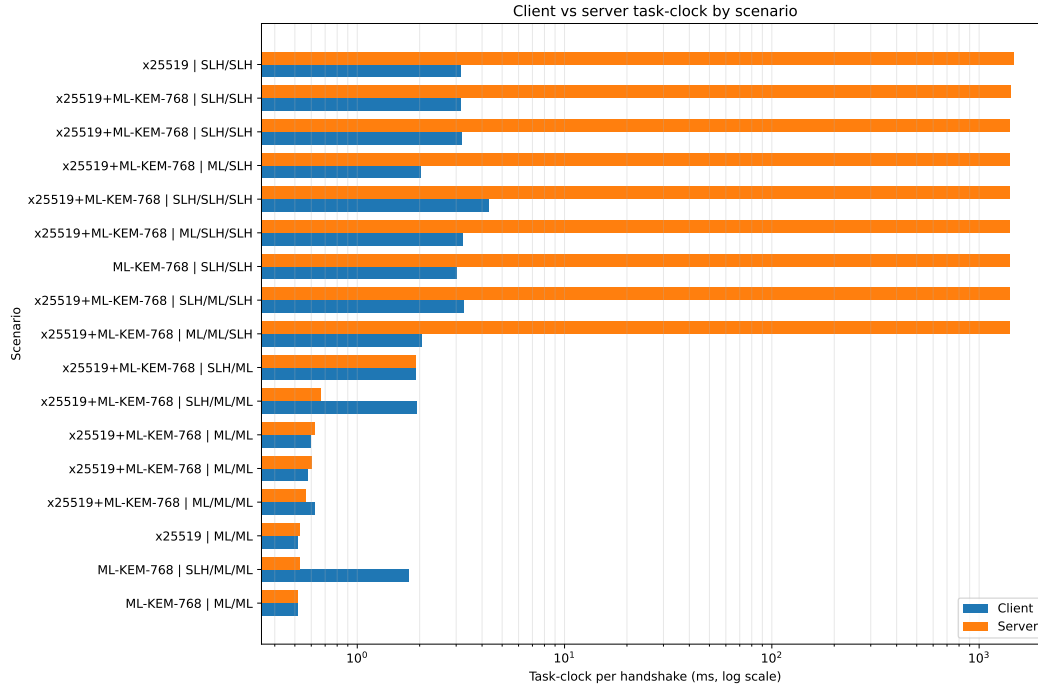


Figure 14: Client versus server task-clock by scenario.

8.3 Validation-skewed regime in upper-layer SLH scenarios

The next distinct regime is formed by scenarios in which SLH-DSA appears in upper trust layers while the interactive leaf remains ML-DSA. These are precisely the cases that carry a visible performance penalty while remaining operationally plausible. Their decomposition reveals that the penalty is not distributed symmetrically.

For the `root-SLH / leaf-ML` class, mean client task-clock rises to approximately 1.8708 ms, whereas mean server task-clock rises only to about 1.0364 ms. When normalized by elapsed time, the client contributes approximately 0.8032 of elapsed time in active work, while the server contributes only about 0.3866. The mean server/client task-clock ratio falls to approximately 0.5477, and the mean instruction ratio to about 0.4360.

This is not a server-collapse pattern. It is a validation-skewed one. The server does more work than in the all-ML baseline, but the relative burden shifts more strongly toward the client. The most natural interpretation is that placing SLH-DSA above the leaf increases the validation burden visible on the client side without forcing the interactive server-authentication step itself into the catastrophic regime.

This distinction is easiest to appreciate when contrasted with the full strategy matrix. The `x25519mlkem768__slh_root__ml_int__ml_leaf` strategy is materially slower than the fully-ML baseline, but it does not resemble the leaf-SLH cases in workload structure. In geometric terms, these scenarios move away from the parity cluster without entering the vertically separated server-dominated cloud shown in Figure 15. That difference is one of the clearest indications that upper-layer SLH and leaf-SLH are not merely stronger and weaker versions of the same phenomenon.

8.4 Overwhelmingly server-bound regime in leaf-SLH scenarios

The decisive result of the decomposition appears once SLH-DSA reaches the leaf. In that class, mean client task-clock is only about 3.0402 ms, while mean server task-clock rises to approximately 1410.8409 ms. The normalized ratios are even more revealing: the client contributes only about 0.0022 of elapsed time in active work, whereas the server contributes about 0.9984. The mean

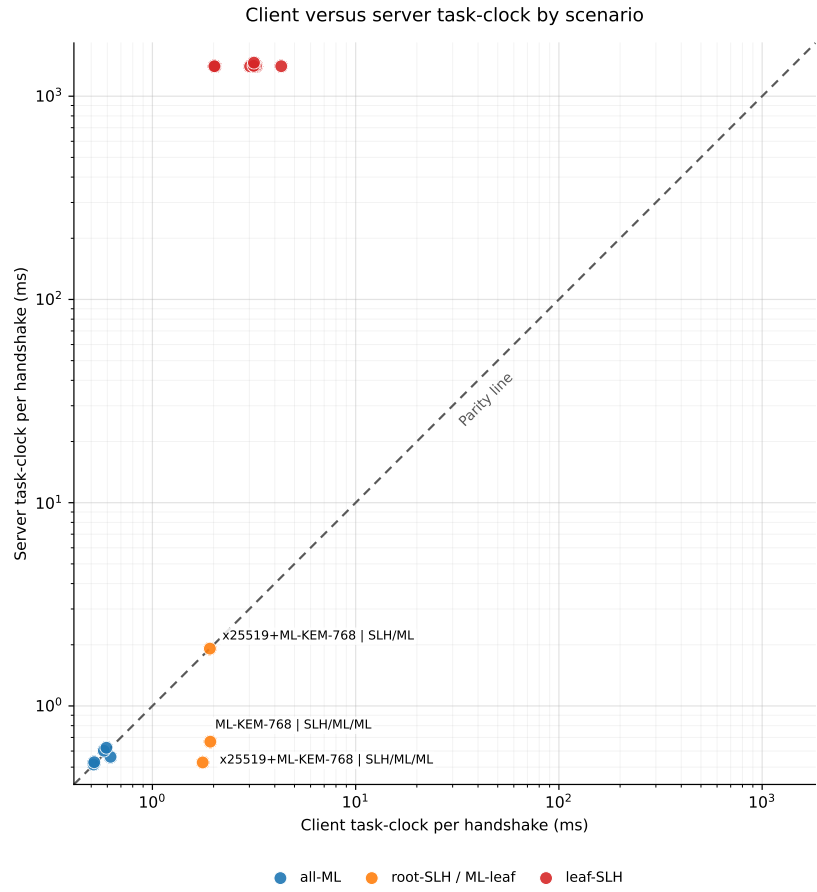


Figure 15: Client versus server task-clock by scenario on log-log axes. The diagonal marks parity between client-side and server-side active work; the clustered separation reveals distinct authentication regimes.

server/client task-clock ratio is approximately 487.95, and the mean server/client instruction ratio is approximately 648.91.

This is no longer simply an expensive handshake. It is an overwhelmingly server-bound one. Figure 13 shows that server-side task-clock explodes only in the leaf-SLH cases. Figure 15 shows the corresponding geometric separation: leaf-SLH scenarios form a distinct cloud far above the client/server parity line rather than a gradual extension of the low-cost region. Figure 16 makes the same point even more directly: in those scenarios, server task-clock almost coincides with end-to-end elapsed time. In practical terms, the total handshake duration is almost entirely accounted for by server-side active compute, while the client is reduced largely to a waiting role.

Figure 17 offers an even harsher summary. Ratios in leaf-SLH scenarios jump from near-unity or sub-unity values into the hundreds. Some of the most extreme cases show server/client task-clock ratios above 680 and instruction ratios above 1000. The handshake is therefore not merely imbalanced; it is dominated by server-side work to an extent that marks a clear regime change.

Among the most server-dominated scenarios are `x25519mlkem768__slh_root__ml_int__slh_leaf`, `x25519mlkem768__ml_root__ml_int__slh_leaf`, and `x25519mlkem768__ml_root__slh_leaf`, all of which exhibit `server_taskclock_over_elapsed` ratios around 0.999 together with enormous server/client asymmetries. The decomposition therefore sharpens the central claim of the paper into a causal statement: the collapse observed in leaf-SLH scenarios is neither primarily a transport phenomenon nor primarily a client-validation phenomenon. It is overwhelmingly a server-side cryptographic compute phenomenon concentrated in the live authentication path.

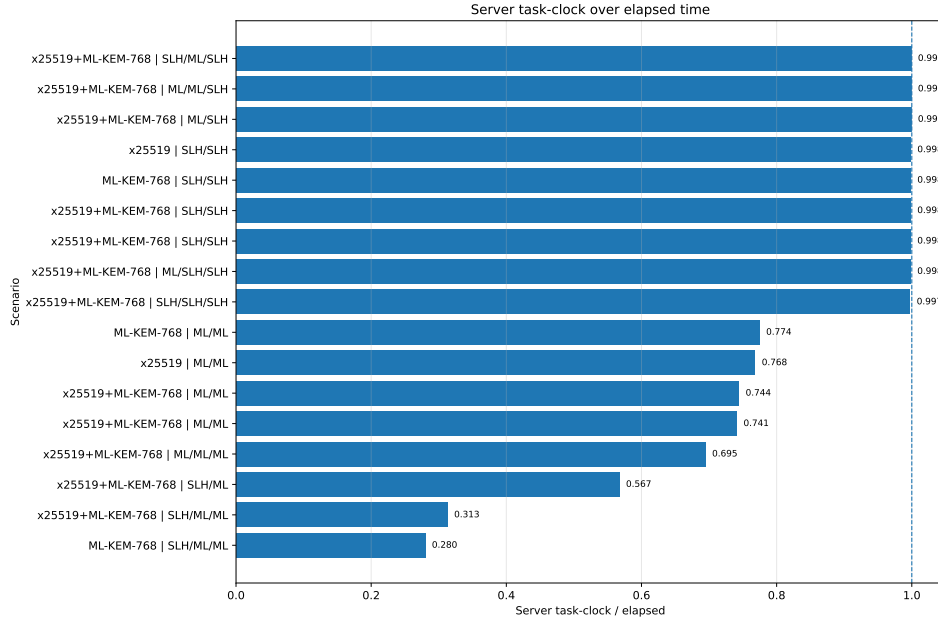


Figure 16: Server task-clock over elapsed time.

8.5 Supporting microarchitectural signals

The dataset also includes lower-level counters such as IPC, cache-miss rate, and branch-miss rate. These should be interpreted cautiously. The present study is not a function-tracing or microarchitectural reverse-engineering exercise, and these counters are used here only as supporting evidence for regime differentiation rather than as proof of a unique internal mechanism.

With that caution in place, the counters still suggest that the heavy leaf-SLH regime is not merely more of the same workload. In the low-cost ML scenarios, the server tends to operate in a comparatively modest regime, with IPC values around 2.1–2.35 and cache-miss rates in the low single-digit range. By contrast, the heavy leaf-SLH scenarios exhibit a stable and sharply separated profile, with server IPC around 4.54–4.55, cache-miss rates roughly in the 33–40% range, and branch-miss rates around 0.48–0.51%.

The appropriate conclusion is deliberately modest. The paper does not claim to identify a single internal OpenSSL or provider function as the unique source of cost, nor to reconstruct the complete internal execution path. The defensible point is narrower and still important: the leaf-SLH cases exhibit a stable server-side execution profile that is sharply distinct from the low-cost ML regime. This reinforces the interpretation already supported by latency, transport, and task-clock decomposition.

Taken together, the decomposition results complete the causal arc of the paper. The previous section showed that leaf-SLH defines a distinct authentication regime insufficiently explained by transport. The present section shows why: once SLH-DSA reaches the server leaf, the handshake becomes almost entirely a server-side compute event. That finding provides the bridge from hierarchy design to deployment consequence and prepares the next step of the argument, namely the translation of authentication cost into capacity loss and operational viability.

9 Operational Implications for PQ TLS Deployment

The previous sections showed that the dominant heavy regime is overwhelmingly server-side and concentrated in leaf-SLH scenarios. The next question is therefore operational rather than merely descriptive: what does that regime imply for a service operator? More precisely, how should second-scale server-authentication cost be translated into capacity loss, infrastructure scaling, and deployment plausibility?

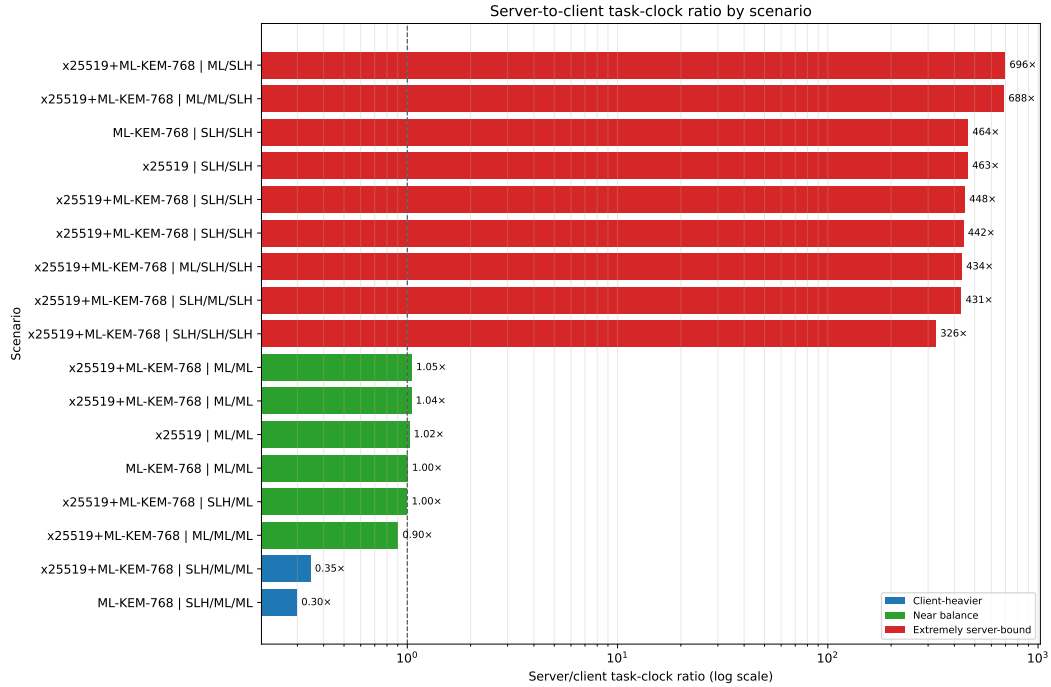


Figure 17: Server-to-client task-clock ratio by scenario.

9.1 From server-side handshake cost to service capacity

For an interactive TLS service, handshake cost is not only a latency issue. It is also a capacity issue. Every additional unit of server-side work per handshake reduces the number of sessions a node can sustain over time, lowers effective throughput per core, and increases the infrastructure required to maintain a fixed service rate. In high-volume settings, these effects accumulate quickly: what appears as a per-handshake cryptographic penalty becomes a constraint on concurrency, scaling, and operational headroom.

This is why the paper moves beyond raw latency. Once the client/server decomposition showed that the heavy regime is overwhelmingly server-side, the relevant unit of interpretation became server CPU time per handshake. From that point onward, the translation to service capacity is direct. If one authentication strategy consumes orders of magnitude more server compute per handshake than another, then throughput per node falls proportionally, and sustaining the same rate of authenticated connections requires proportionally more capacity.

In that sense, the heavy leaf-SLH regime is not merely a slower version of certificate-based TLS. It is a cryptographic authentication design that consumes server compute in a way that directly constrains deployable scale. For an operator, the relevant question is therefore not whether the handshake remains formally correct, but whether it remains operationally viable at the service layer.

9.2 Capacity loss under leaf-SLH

The most direct operational translation of the server-side measurements is handshake capacity. Table 11 reports derived capacity metrics such as handshakes per core-second, handshakes per vCPU-hour, retained capacity relative to baseline, and the infrastructure multiplier required to preserve baseline throughput.

The hybrid depth-3 fully-ML baseline, `x25519mlkem768_ml_root_ml_int_ml_leaf`, supports approximately 1779.68 handshakes per core-second, or about 6,406,856.76 handshakes per vCPU-hour. This is the reference point against which the remaining strategies are interpreted.

Table 10: Performance decomposition summary.

scenario_id	elapsed_mean_ms	client_task_clock_per_run_ms	server_task_clock_per_run_ms	client_taskclock_over_elapsed
mlkem768_ml_root_ml_leaf	0.665200	0.513600	0.515200	0.772100
mlkem768_slh_root_ml_int_ml_leaf	1.884200	1.767500	0.527300	0.938100
mlkem768_slh_root_slh_leaf	1405.455900	3.024100	1402.896000	0.002200
x25519_leaf_mlds65	0.688500	0.517300	0.528700	0.751400
x25519_leaf_slhdsashake192s	1464.932700	3.159200	1462.281300	0.002200
x25519mlkem768_leaf_mlds65	0.840600	0.593700	0.622800	0.706200
x25519mlkem768_leaf_slhdsashake192s	1413.991400	3.148500	1411.344800	0.002200
x25519mlkem768_ml_root_ml_int_ml_leaf	0.809100	0.622200	0.561900	0.769000
x25519mlkem768_ml_root_ml_int_slh_leaf	1402.486200	2.036700	1401.169400	0.001500
x25519mlkem768_ml_root_ml_leaf	0.809300	0.576800	0.602200	0.712700
x25519mlkem768_ml_root_slh_int_slh_leaf	1405.802800	3.235800	1403.109500	0.002300
x25519mlkem768_ml_root_slh_leaf	1406.283200	2.018000	1404.926900	0.001400
x25519mlkem768_slh_root_ml_int_ml_leaf	2.133000	1.927300	0.667200	0.903600
x25519mlkem768_slh_root_ml_int_slh_leaf	1403.165900	3.254300	1401.849300	0.002300
x25519mlkem768_slh_root_ml_leaf	3.376200	1.917600	1.914600	0.568000
x25519mlkem768_slh_root_slh_int_slh_leaf	1408.703300	4.303500	1404.903400	0.003100
x25519mlkem768_slh_root_slh_leaf	1407.714100	3.182100	1405.087400	0.002300

scenario_id	server_taskclock_over_elapsed	server_client_taskclock_ratio	qualitative_perf_regime
mlkem768_ml_root_ml_leaf	0.774500	1.003000	balanced
mlkem768_slh_root_ml_int_ml_leaf	0.279800	0.298300	client_skewed
mlkem768_slh_root_slh_leaf	0.998200	463.910400	overwhelmingly_server_bound
x25519_leaf_mlds65	0.768000	1.022100	balanced
x25519_leaf_slhdsashake192s	0.998200	462.869300	overwhelmingly_server_bound
x25519mlkem768_leaf_mlds65	0.741000	1.049200	balanced
x25519mlkem768_leaf_slhdsashake192s	0.998100	448.264200	overwhelmingly_server_bound
x25519mlkem768_ml_root_ml_int_ml_leaf	0.694500	0.903100	balanced
x25519mlkem768_ml_root_ml_int_slh_leaf	0.999100	687.949400	overwhelmingly_server_bound
x25519mlkem768_ml_root_ml_leaf	0.744100	1.044100	balanced
x25519mlkem768_ml_root_slh_int_slh_leaf	0.998100	433.616100	overwhelmingly_server_bound
x25519mlkem768_ml_root_slh_leaf	0.999000	696.186200	overwhelmingly_server_bound
x25519mlkem768_slh_root_ml_int_ml_leaf	0.312800	0.346200	client_skewed
x25519mlkem768_slh_root_ml_int_slh_leaf	0.999100	430.763900	overwhelmingly_server_bound
x25519mlkem768_slh_root_ml_leaf	0.567100	0.998500	balanced
x25519mlkem768_slh_root_slh_int_slh_leaf	0.997300	326.456000	overwhelmingly_server_bound
x25519mlkem768_slh_root_slh_leaf	0.998100	441.559800	overwhelmingly_server_bound

The all-ML family remains essentially aligned with that baseline. Its mean retained capacity is approximately $0.9977\times$ baseline, and its mean infrastructure multiplier is approximately $1.0076\times$. In practical terms, the all-ML region is capacity-stable.

The root-SLH / leaf-ML family introduces a real but bounded degradation. Its mean retained capacity is approximately $0.7338\times$ baseline, implying a mean infrastructure multiplier of approximately $1.8444\times$, with a much more moderate median multiplier of approximately $1.1874\times$. This is not negligible, but it remains within a range that could be tolerated in some deployment contexts, especially where a heavier upper trust layer is judged worthwhile.

The leaf-SLH class behaves very differently. Its mean retained capacity falls to approximately $0.0004\times$ baseline, and its mean infrastructure multiplier reaches approximately $2510.85\times$, with a median around $2500.28\times$. Figure 18 makes the scale of this discontinuity immediately visible. The leaf-SLH scenarios do not sit somewhat above the baseline; they stand several orders of magnitude beyond it.

At that point, the architectural distinction becomes operationally unavoidable. A configuration that requires on the order of $2500\times$ more infrastructure to preserve baseline throughput cannot reasonably be described as merely less efficient. It belongs to a different deployment class altogether. The language of bounded penalty no longer applies; what appears instead is a collapse of handshake throughput as a practical front-end primitive.

9.3 Cost-per-million-handshakes interpretation

Capacity loss is already an infrastructure result, but a second useful translation is cost per million handshakes. This metric is especially helpful because it is portable across traffic scales, easy to compare, and directly tied to per-handshake server burden.

Table 12 and Figure 19 summarize this view. Under the illustrative price model used in the analysis, the fully-ML baseline costs approximately 0.006243 per million handshakes. The root-SLH / ml_int / ml_leaf strategy rises only modestly, to approximately 0.007413 per million, for an extra cost of about 0.001170 and a cost multiplier of about $1.187\times$.

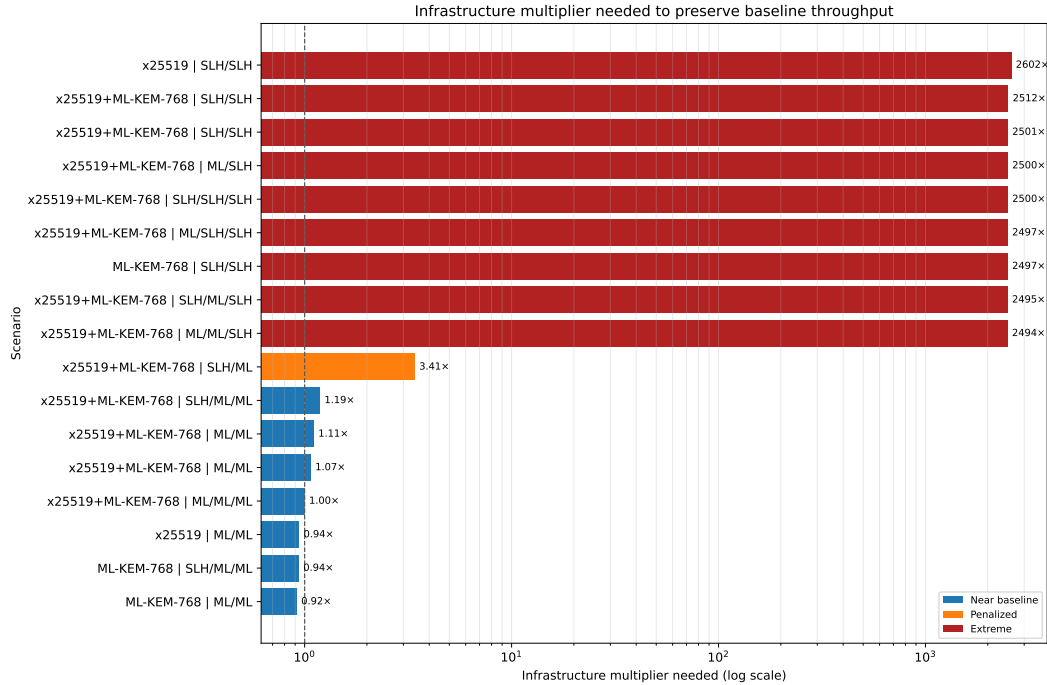


Figure 18: Infrastructure multiplier needed to preserve baseline throughput.

The leaf-SLH cases, by contrast, expand economically in direct parallel with their compute behavior. Representative heavy scenarios such as `x25519mlkem768__slh_root__slh_int__slh_leaf` and `x25519mlkem768__ml_root__slh_leaf` land around 15.61 cost units per million handshakes, yielding extra costs above 15.60 relative to baseline and cost multipliers near 2500×. The most extreme observed case, `x25519__leaf_slhdsashake192s`, reaches approximately 16.247570 per million handshakes, or about 2602.396× the baseline.

This metric is not presented as an accounting statement about any one provider bill. Its value lies elsewhere. It compresses the operational meaning of the measured server-side cost into a quantity that remains intelligible across contexts. In that representation, upper-layer SLH appears as a bounded premium. Leaf-SLH appears as a structural distortion of the baseline rather than as an expensive but ordinary variant.

9.4 Service-class translation

Cost per million handshakes is portable, but operators often reason in deployment classes rather than in normalized per-million metrics. For that reason, the analysis also expresses the economic model through three illustrative service classes: `small_internal`, `medium_api`, and `high_volume_frontend`. These classes are not intended as universal thresholds, but as a concrete way of showing how the same cryptographic design decision changes meaning as traffic scale increases.

Table 13 and Figure 20 present that translation. Under the illustrative assumptions of the model, the median extra monthly cost of the `root-SLH / leaf-ML` class remains small: around 0.0035 for a small internal service, around 0.3509 for a medium API, and around 3.5092 for a high-volume front-end. This is fully consistent with the bounded-penalty interpretation developed in the earlier sections.

The leaf-SLH class behaves very differently. Its median extra monthly cost rises from approximately 46.8114 in the small internal service class to about 4681.1385 in the medium API class and about 46811.3845 in the high-volume front-end class. The scaling pattern itself is unsurprising, since the model is linear in traffic. What matters is its meaning. A decision that may look merely expensive in a

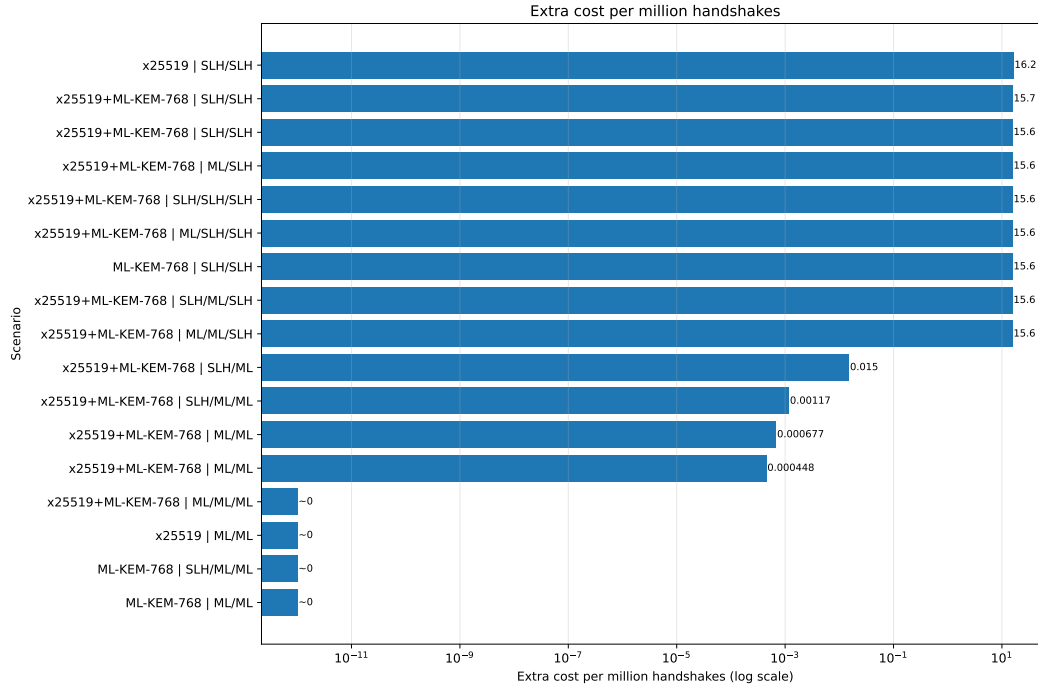


Figure 19: Extra cost per million handshakes.

low-volume setting becomes economically grotesque in an edge-facing or high-throughput interactive deployment.

This is the point at which the paper’s hierarchy argument becomes fully operational. The same certificate strategy can have very different practical meaning depending on service class. A bounded premium in an upper-layer SLH design may remain tolerable across multiple environments. The discontinuity introduced by leaf-SLH, however, scales directly into a front-end deployment problem.

9.5 Operational plausibility of hierarchy strategies

The final step is to restate the results in explicitly operational terms. Earlier in the paper, the strategy space was described through four classes: *Reasonable*, *Penalized but plausible*, *Operationally problematic*, and *Unsuitable for interactive TLS front-end*. That language is not ornamental. It is the appropriate summary once latency, workload concentration, capacity loss, and economic translation are considered together.

The all-ML strategies remain firmly in the *Reasonable* class. They are low-latency, structurally balanced, capacity-stable, and economically aligned with the baseline. The root-SLH / intermediate-ML / leaf-ML strategy belongs in *Penalized but plausible*. It introduces a real cost in latency, capacity, and deployment overhead, but remains within a bounded interactive regime. In contexts that value a heavier upper trust layer, that premium may be acceptable.

The leaf-SLH strategies do not belong to the same continuum. Their latency plateau, server-bound compute profile, capacity collapse, infrastructure multipliers, and cost expansion all point in the same direction. In low-volume settings one may still tolerate them for reasons outside performance, but from the perspective of interactive service engineering they belong in the *Unsuitable* class. The heavy regime is not merely suboptimal. It is operationally disqualifying for front-end TLS use.

This is precisely the sort of conclusion that a flat algorithm benchmark cannot provide. A flat benchmark can say that one signature scheme is slower or larger than another. The present study can say something stronger and more useful: which certificate-hierarchy strategies remain deployable,

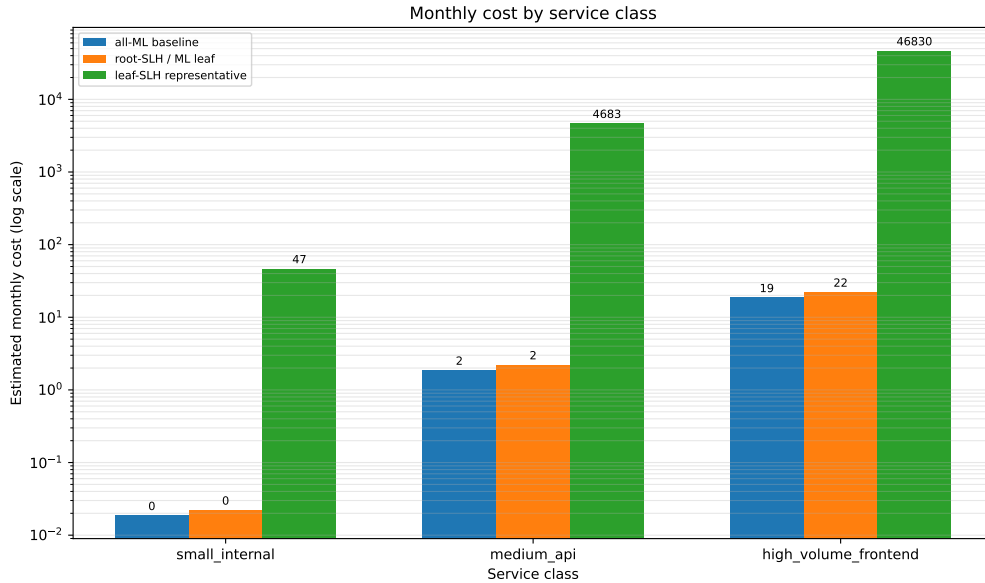


Figure 20: Monthly cost by service class.

which impose bounded strategic premiums, and which turn server authentication into a scaling pathology.

10 Threats to Validity and Limitations

The conclusions of this paper are strong within the experimental setting studied, but they should not be read as universal statements about every possible TLS implementation, network environment, or post-quantum deployment model. Several limitations therefore deserve explicit discussion.

10.1 Local execution environment

All measurements were collected in a controlled local environment, with the final dataset generated on bare metal rather than over a wide-area network. This is both a strength and a limitation. It is a strength because it reduces network noise and allows certificate-path effects, chain exposure, and client/server cryptographic burden to be isolated more cleanly. It is a limitation because it does not capture WAN latency, Internet path variability, queuing under production concurrency, or deployment-specific interactions with middleboxes and edge infrastructure.

Accordingly, the latency values reported here should not be interpreted as direct predictions of end-user Internet latency under arbitrary operating conditions. Their role is comparative rather than predictive: they characterize how different certificate-hierarchy strategies behave within a real implementation stack under controlled conditions. That is precisely the level required to isolate hierarchy-sensitive authentication effects, but it remains narrower than full deployment forecasting.

10.2 Single implementation stack

The study is conducted on a specific implementation stack, namely OpenSSL 3 together with oqsprovider and liboqs. This choice is deliberate and technically justified, but it also means that the results are implementation-dependent. Different TLS libraries, certificate-handling paths, provider integrations, or post-quantum implementations could shift absolute values and potentially alter some lower-level trade-offs.

For that reason, the strongest claims of the paper are structural rather than universal. The paper does not claim that every TLS implementation would produce exactly the same ratios or absolute timings. It claims instead that, within a serious real-stack setting, hierarchy-sensitive signature placement can

Table 11: Infrastructure capacity summary.

scenario_id	kex_mode	depth	handshakes_per_core_second	handshakes_per_vcpu_hour	capacity_retained_vs_baseline
mlkem768__ml_root__ml_leaf	pure_pqc	2	1,940.97	6,987,482.70	1.0906
mlkem768__slh_root__ml_int__ml_leaf	pure_pqc	3	1,896.59	6,827,725.12	1.0657
x25519__leaf__mlds65	classical	2	1,891.31	6,808,716.67	1.0627
x25519mlkem768__ml_root__ml_int__ml_leaf	hybrid	3	1,779.68	6,406,856.76	1.0000
x25519mlkem768__ml_root__ml_leaf	hybrid	2	1,660.56	5,978,030.74	0.9331
x25519mlkem768__leaf__mlds65	hybrid	2	1,605.53	5,779,919.92	0.9021
x25519mlkem768__slh_root__ml_int__ml_leaf	hybrid	3	1,498.86	5,395,885.64	0.8422
x25519mlkem768__slh_root__ml_leaf	hybrid	2	522.29	1,880,240.19	0.2935
x25519mlkem768__ml_root__ml_int__slh_leaf	hybrid	3	0.71	2,569.28	0.0004
x25519mlkem768__slh_root__ml_int__slh_leaf	hybrid	3	0.71	2,568.04	0.0004
mlkem768__slh_root__slh_leaf	pure_pqc	2	0.71	2,566.12	0.0004
x25519mlkem768__ml_root__slh_int__slh_leaf	hybrid	3	0.71	2,565.73	0.0004
x25519mlkem768__slh_root__slh_int__slh_leaf	hybrid	3	0.71	2,562.45	0.0004
x25519mlkem768__ml_root__slh_leaf	hybrid	2	0.71	2,562.41	0.0004
x25519mlkem768__slh_root__slh_leaf	hybrid	2	0.71	2,562.12	0.0004
x25519mlkem768__leaf__slhdsashake192s	hybrid	2	0.71	2,550.76	0.0004
x25519__leaf__slhdsashake192s	classical	2	0.68	2,461.91	0.0004

scenario_id	kex_mode	infrastructure_multiplier_needed	conceptual_perf_group
mlkem768__ml_root__ml_leaf	pure_pqc	0.9169	all_ml
mlkem768__slh_root__ml_int__ml_leaf	pure_pqc	0.9384	root_slh_leaf_ml
x25519__leaf__mlds65	classical	0.9410	all_ml
x25519mlkem768__ml_root__ml_int__ml_leaf	hybrid	1.0000	all_ml
x25519mlkem768__ml_root__ml_leaf	hybrid	1.0717	all_ml
x25519mlkem768__leaf__mlds65	hybrid	1.1085	all_ml
x25519mlkem768__slh_root__ml_int__ml_leaf	hybrid	1.1874	root_slh_leaf_ml
x25519mlkem768__slh_root__ml_leaf	hybrid	3.4075	root_slh_leaf_ml
x25519mlkem768__ml_root__ml_int__slh_leaf	hybrid	2493.6366	leaf_slh
x25519mlkem768__slh_root__ml_int__slh_leaf	hybrid	2494.8466	leaf_slh
mlkem768__slh_root__slh_leaf	pure_pqc	2496.7094	leaf_slh
x25519mlkem768__ml_root__slh_int__slh_leaf	hybrid	2497.0893	leaf_slh
x25519mlkem768__slh_root__slh_int__slh_leaf	hybrid	2500.2820	leaf_slh
x25519mlkem768__ml_root__slh_leaf	hybrid	2500.3237	leaf_slh
x25519mlkem768__slh_root__slh_leaf	hybrid	2500.6093	leaf_slh
x25519mlkem768__leaf__slhdsashake192s	hybrid	2511.7455	leaf_slh
x25519__leaf__slhdsashake192s	classical	2602.3964	leaf_slh

Table 12: Economic summary by scenario/class.

scenario_id	conceptual economic class	server CPU seconds per handshake	handshakes per server CPU second	handshakes per server CPU hour	capacity retained vs baseline	capacity loss vs baseline (%)	infrastructure multiplier needed
x25519mlkem768__ml_root__ml_int__ml_leaf	all_ml	0.0006	1779.6824	6406856.7605	1.0000	0.0000	1.0000
x25519mlkem768__slh_root__ml_int__ml_leaf	root_slh_leaf_ml	0.0007	1498.8571	5395885.6372	0.8422	15.7795	1.1874
x25519mlkem768__slh_root__slh_int__slh_leaf	leaf_slh	1.4049	0.7118	2562.4537	0.0004	99.9600	2500.2820
x25519mlkem768__ml_root__slh_int__slh_leaf	leaf_slh	1.4049	0.7118	2562.4109	0.0004	99.9600	2500.3237
x25519__leaf__slhdsashake192s	leaf_slh	1.4623	0.6839	2461.9066	0.0004	99.9616	2602.3964

scenario_id	conceptual economic class	CPU hours per million handshakes	cost per million default	extra cost per million default	cost multiplier vs baseline
x25519mlkem768__ml_root__ml_int__ml_leaf	all_ml	0.1561	0.0062	0.0000	1.0000
x25519mlkem768__slh_root__ml_int__ml_leaf	root_slh_leaf_ml	0.1853	0.0074	0.0012	1.1874
x25519mlkem768__slh_root__slh_int__slh_leaf	leaf_slh	390.2510	15.6100	15.6038	2500.2820
x25519mlkem768__ml_root__slh_int__slh_leaf	leaf_slh	390.2575	15.6103	15.6041	2500.3237
x25519__leaf__slhdsashake192s	leaf_slh	406.1893	16.2476	16.2413	2602.3964

dominate the operational cost of post-quantum TLS authentication to an extent that flat algorithm comparisons fail to capture.

10.3 Semantics of observed chain exposure

A recurring methodological subtlety throughout the paper is that the effective chain observed by the client is not always equivalent to the naive logical PKI topology. In the dataset ana-

Table 13: Service-class economic translation.

service class	conceptual economic class	scenarios	mean daily cost	median daily cost	mean extra daily cost vs baseline	median extra daily cost vs baseline	mean monthly cost (30d)	median monthly cost (30d)
high_volume_frontend	all_ml	5	0.6291	0.6243	0.0048	0.0000	18.8726	18.7299
high_volume_frontend	leaf_slh	9	1567.6010	1561.0038	1566.9767	1560.3795	47028.0298	46830.1144
high_volume_frontend	root_slh_leaf_ml	3	1.1515	0.7413	0.5272	0.1170	34.5454	22.2392
medium_api	all_ml	5	0.0629	0.0624	0.0005	0.0000	1.8873	1.8730
medium_api	leaf_slh	9	156.7601	156.1004	156.6977	156.0379	4702.8030	4683.0114
medium_api	root_slh_leaf_ml	3	0.1152	0.0741	0.0527	0.0117	3.4545	2.2239
small_internal	all_ml	5	0.0006	0.0006	0.0000	0.0000	0.0189	0.0187
small_internal	leaf_slh	9	1.5676	1.5610	1.5670	1.5604	47.0280	46.8301
small_internal	root_slh_leaf_ml	3	0.0012	0.0007	0.0005	0.0001	0.0345	0.0222

service class	conceptual economic class	scenarios	mean extra monthly cost (30d) vs baseline	median extra monthly cost (30d) vs baseline	mean annual cost (365d)	mean extra annual cost (365d) vs baseline
high_volume_frontend	all_ml	5	0.1427	0.0000	229.6166	1.7358
high_volume_frontend	leaf_slh	9	47009.2998	46811.3845	572174.3620	571946.4811
high_volume_frontend	root_slh_leaf_ml	3	15.8155	3.5092	420.3024	192.4215
medium_api	all_ml	5	0.0143	0.0000	22.9617	0.1736
medium_api	leaf_slh	9	4700.9300	4681.1385	57217.4362	57194.6481
medium_api	root_slh_leaf_ml	3	1.5815	0.3509	42.0302	19.2422
small_internal	all_ml	5	0.0001	0.0000	0.2296	0.0017
small_internal	leaf_slh	9	47.0093	46.8114	572.1744	571.9465
small_internal	root_slh_leaf_ml	3	0.0158	0.0035	0.4203	0.1924

lyzed here, `chain_len_unique = 2` does not imply that the hierarchy is logically depth 2, and `served_chain_der_bytes` does not carry fully homogeneous semantics across all topology classes.

This is not a flaw in the data, but it does impose interpretive discipline. For that reason, the paper relies primarily on `bytes_read_mean` and `chain_bytes_unique` for strict cross-depth transport reasoning, and treats `served_chain_der_bytes` with explicit caution. The consequence is that some chain-level conclusions must be stated in empirical rather than idealized PKI terms. That is appropriate for a deployment-oriented study, but it remains a limitation relative to fully instrumented protocol tracing or implementation-level certificate-path introspection.

10.4 Perf as proxy rather than full function tracing

The client/server performance-counter analysis is one of the strongest components of the paper, but it remains aggregate evidence rather than full internal function tracing. The results show clearly that leaf-SLH scenarios are overwhelmingly server-side and nearly compute-bound at the server, but they do not by themselves identify a unique internal function, call path, or provider-level routine as the exclusive source of cost.

This matters especially for the microarchitectural discussion. IPC, cache-miss, and branch-miss patterns strongly suggest that the heavy leaf-SLH regime is structurally distinct from the all-ML regime, but the paper does not claim to reconstruct the precise internal execution path of OpenSSL or oqsprovider. The performance-counter evidence is therefore best interpreted as regime-level causal support rather than as proof of a uniquely identified internal mechanism.

10.5 Economic model as derived interpretation

The economic section of the paper is intentionally framed as an operational interpretation derived from measured server-side compute cost. The service classes, pricing assumptions, and cost-per-million-handshakes figures are illustrative and parameterized rather than tied to a specific commercial contract, cloud provider invoice, or production deployment profile.

The paper should therefore not be read as providing the exact future bill of any particular organization. Its contribution is different. It translates measured authentication cost into a portable capacity-based and compute-based language that makes deployment consequences easier to reason about across contexts. That portability is the strength of the model, but it also defines its limit: it is an interpretation layer, not an accounting statement.

Taken together, these limitations do not invalidate the paper’s central findings. They define their scope. The paper does not claim universal deployment prophecy. It claims that, in a realistic local TLS stack with structured hierarchy variation and measured client/server workload, signature placement decisively shapes the operational viability of post-quantum TLS authentication.

11 Conclusion

11.1 Main finding

The main finding of this paper is that post-quantum migration in TLS 1.3 is best understood as a certificate-hierarchy design problem rather than as a flat comparison between signature algorithms. Across all four campaigns, the most important practical distinction is not whether SLH-DSA appears somewhere in the certification path, but whether it reaches the handshake-exposed server leaf.

Once that happens, the authentication path enters a qualitatively different regime. Mean latency moves from the sub-millisecond or low-millisecond region into the ~ 1.4 -second range, server-side active compute becomes almost identical to end-to-end elapsed time, retained capacity collapses, and infrastructure multipliers rise by orders of magnitude. By contrast, scenarios that confine SLH-DSA to upper trust layers while preserving ML-DSA in the interactive leaf remain within a bounded and materially more plausible regime.

The paper therefore supports a precise conclusion: the operational meaning of a post-quantum signature family in TLS is not determined by its mere presence in the hierarchy, but by its placement within the live authentication path.

11.2 Implications for certificate hierarchy design

This conclusion has direct implications for the design of post-quantum certificate hierarchies. A migration strategy should not be evaluated only in terms of standardization status, primitive-level conservatism, or conceptual uniformity across the entire PKI. It must also be evaluated in terms of which certificates are exposed during the handshake and where the resulting cryptographic burden is paid.

The results suggest that uniform post-quantum placement across the whole hierarchy is not necessarily the most rational deployment strategy. In particular, the data support a more selective approach in which heavier signature families may be tolerated in upper trust layers while the interactive server leaf is protected from the regime-defining cost of SLH-DSA. Within the design space studied here, `root-SLH / intermediate-ML / leaf-ML` emerges as a materially penalized but still plausible strategy, whereas `leaf-SLH` configurations do not remain in the same operational class.

More broadly, the study shows that effective chain exposure is part of the design problem itself. Logical hierarchy depth, declared certificate structure, and practical handshake exposure cannot be treated as interchangeable notions. In post-quantum TLS authentication, hierarchy design is not merely administrative PKI arrangement. It is part of the cryptographic surface of the protocol.

11.3 What remains open

Several lines of work remain open. First, the present study uses a single implementation stack. Repeating the same hierarchy-sensitive analysis across other TLS libraries and post-quantum integrations would strengthen confidence in the generality of the structural findings. Second, the present work focuses on full handshakes rather than resumed sessions. Session resumption may alter the practical weight of certificate-path cost in some real deployment settings.

Third, the analysis could be extended to other protocol settings in which certificate-based authentication remains central. QUIC is an especially important case, given its deployment relevance and its close relationship to TLS 1.3. Additional work could also explore WAN-based measurements, more detailed implementation tracing, and sector-specific trust models in which upper-layer certificate choices are constrained by regulatory or long-lived trust-anchor considerations.

Finally, the broader post-quantum transition raises a more general design question that goes beyond the specific scenarios measured here: how should protocol designers and operators distribute cryptographic conservatism across the certification hierarchy when different positions in that hierarchy have radically different operational meaning? The present paper does not settle that question in general, but it does show that answering it requires more than flat primitive comparison.

11.4 Final closing statement

The relevant question is not whether post-quantum signatures can be embedded into TLS 1.3, but which certificate placements preserve authenticated key establishment without turning server authentication into a cryptographic scaling pathology.

References

- [1] David Cooper et al. *Internet X.509 Public Key Infrastructure Certificate and Certificate Revocation List (CRL) Profile*. RFC 5280. May 2008. DOI: 10.17487/RFC5280. URL: <https://www.rfc-editor.org/rfc/rfc5280.html>.
- [2] P. Kampanakis, S. Fluhrer, et al. *Post-Quantum Cryptography Recommendations for Application Services*. IETF Internet-Draft, draft-ietf-uta-pqc-app. Feb. 2026. URL: <https://datatracker.ietf.org/doc/draft-ietf-uta-pqc-app/>.
- [3] J. A. Montenegro et al. *A Performance Evaluation Framework for Post-Quantum TLS*. University of Málaga technical paper / preprint. 2025. URL: <https://www.nics.uma.es/wp-content/papers/Monte2025pqc.pdf>.
- [4] National Institute of Standards and Technology. *Module-Lattice-Based Digital Signature Standard*. Tech. rep. FIPS 204. U.S. Department of Commerce, Aug. 2024. URL: <https://nvlpubs.nist.gov/nistpubs/fips/nist.fips.204.pdf>.
- [5] National Institute of Standards and Technology. *Module-Lattice-Based Key-Encapsulation Mechanism Standard*. Tech. rep. FIPS 203. U.S. Department of Commerce, Aug. 2024. URL: <https://nvlpubs.nist.gov/nistpubs/fips/nist.fips.203.pdf>.
- [6] National Institute of Standards and Technology. *Stateless Hash-Based Digital Signature Standard*. Tech. rep. FIPS 205. U.S. Department of Commerce, Aug. 2024. URL: <https://nvlpubs.nist.gov/nistpubs/fips/nist.fips.205.pdf>.
- [7] Open Quantum Safe Project. *liboqs*. <https://openquantumsafe.org/liboqs/>. Accessed 2026-03-23. 2026.
- [8] Open Quantum Safe Project. *OpenSSL 3 Provider (OQS Provider)*. <https://openquantumsafe.org/applications/tls.html>. Accessed 2026-03-23. 2026.
- [9] Sebastian Paul et al. *Mixed Certificate Chains for the Transition to Post-Quantum Authentication in TLS 1.3*. Cryptology ePrint Archive, Paper 2021/1447. 2021. URL: <https://eprint.iacr.org/2021/1447>.
- [10] Eric Rescorla. *The Transport Layer Security (TLS) Protocol Version 1.3*. RFC 8446. Aug. 2018. DOI: 10.17487/RFC8446. URL: <https://www.rfc-editor.org/rfc/rfc8446.html>.
- [11] Dimitrios Sikeridis, Panos Kampanakis, and Michael Devetsikiotis. “Post-Quantum Authentication in TLS 1.3: A Performance Study”. In: *Proceedings of the Network and Distributed System Security Symposium (NDSS)*. 2020. URL: <https://www.ndss-symposium.org/wp-content/uploads/2020/02/24203.pdf>.
- [12] D. Stebila et al. *ML-KEM Post-Quantum Key Agreement for TLS 1.3*. IETF Internet-Draft, draft-ietf-tls-mlkem-07. Feb. 2026. URL: <https://datatracker.ietf.org/doc/draft-ietf-tls-mlkem/>.
- [13] Sean Turner, Deirdre Connolly, et al. *Hybrid Key Exchange in TLS 1.3*. IETF Internet-Draft, draft-ietf-tls-hybrid-design-16. Feb. 2026. URL: <https://datatracker.ietf.org/doc/html/draft-ietf-tls-hybrid-design-16>.

A Scenario Inventory

This appendix provides the full experimental inventory used in the study. Its purpose is documentary rather than interpretive. The main text discusses only those scenario distinctions required for causal and operational interpretation, whereas this appendix preserves the broader inventory for traceability and reproducibility.

Scenario identifiers are constructed compositionally. They encode the key-establishment mode together with the signature-family placement across the logical certificate hierarchy. In the naming convention used throughout the paper, `root`, `int`, and `leaf` denote the certificate positions in the hierarchy, while labels such as `m1` and `s1h` denote the corresponding signature-family assignment. Depth-2 scenarios omit the intermediate position by construction.

Table 14: Experimental inventory and scenario matrix.

Campaign	Scenario	TL-S group	Root	Intermediate	Leaf	Depth	Runs
A	x25519__leaf_mlds65	x25519	ML-DSA	—	ML-DSA	2	10000
A	x25519__leaf_slhdsashake192s	x25519	SLH-DSA	—	SLH-DSA	2	300
A	x25519mlkem768__leaf_mlds65	x25519mlkem768	ML-DSA	—	ML-DSA	2	10000
A	x25519mlkem768__leaf_slhdsashake192s	x25519mlkem768	SLH-DSA	—	SLH-DSA	2	300
B	x25519mlkem768__ml_int_ml_leaf	x25519mlkem768	ML-DSA	ML-DSA	ML-DSA	3	10000
B	x25519mlkem768__ml_int_ml_int_slh_leaf	x25519mlkem768	ML-DSA	ML-DSA	SLH-DSA	3	300
B	x25519mlkem768__ml_int_slh_int_slh_leaf	x25519mlkem768	ML-DSA	SLH-DSA	SLH-DSA	3	300
B	x25519mlkem768__slh_root_ml_int_ml_leaf	x25519mlkem768	SLH-DSA	ML-DSA	ML-DSA	3	10000
B	x25519mlkem768__slh_root_ml_int_slh_leaf	x25519mlkem768	SLH-DSA	ML-DSA	SLH-DSA	3	300
B	x25519mlkem768__slh_root_slh_int_slh_leaf	x25519mlkem768	SLH-DSA	SLH-DSA	SLH-DSA	3	300
C	x25519mlkem768__ml_root_ml_leaf	x25519mlkem768	ML-DSA	—	ML-DSA	2	10000
C	x25519mlkem768__ml_root_slh_leaf	x25519mlkem768	ML-DSA	—	SLH-DSA	2	300
C	x25519mlkem768__slh_root_ml_leaf	x25519mlkem768	SLH-DSA	—	ML-DSA	2	10000
C	x25519mlkem768__slh_root_slh_leaf	x25519mlkem768	SLH-DSA	—	SLH-DSA	2	300
D	mlkem768__ml_root_ml_leaf	mlkem768	ML-DSA	—	ML-DSA	2	10000
D	mlkem768__slh_root_ml_int_ml_leaf	mlkem768	SLH-DSA	ML-DSA	ML-DSA	3	10000
D	mlkem768__slh_root_slh_leaf	mlkem768	SLH-DSA	—	SLH-DSA	2	300

B Additional Measurement Notes

This appendix collects methodological clarifications that support interpretation of the dataset but are not essential to the main argumentative flow of the paper.

B.1 Observed chain length versus logical hierarchy depth

In the dataset analyzed here, the observed value `chain_len_unique = 2` does not imply that the logical certification hierarchy has depth 2. The client consistently observes two certificates in the effective chain, but those two certificates do not always correspond to the same logical pair. In depth-2 scenarios, the observed pair may correspond to root plus leaf; in depth-3 scenarios, it may instead correspond to intermediate plus leaf. For that reason, effective chain exposure must be treated as an empirical property of the live handshake rather than inferred directly from the declared PKI structure.

B.2 Semantics of `served_chain_der_bytes`

The variable `served_chain_der_bytes` does not carry identical semantics across all topology classes. In the present dataset, it aligns with leaf DER size in some depth-2 scenarios, whereas in depth-3 scenarios it more closely tracks the observed effective chain. Accordingly, strict cross-depth transport comparisons in the main text rely primarily on `bytes_read_mean` and `chain_bytes_unique`.

B.3 Scenario reuse and deduplication

Some scenarios appear in more than one campaign context by design, especially in the relationship between Campaign B and Campaign C. This is analytical reuse rather than data corruption. For cross-cutting interpretation, the scenario-level dataset is therefore deduplicated by `scenario_id`, while campaign identity is preserved where narratively relevant in the main text.

B.4 Non-uniform sample sizes

Sample sizes were not uniform across scenarios. Fast scenarios were executed with large sample counts, whereas extremely heavy scenarios, particularly those involving SLH-DSA in the leaf, were run with smaller but still analytically sufficient counts. This choice was made deliberately to balance feasibility against statistical stability. Since the paper's main findings concern regime separation and orders-of-magnitude discontinuities rather than marginal effects, this asymmetry does not affect the structural interpretation.

B.5 Use of perf-derived metrics

The performance-counter metrics reported in the paper are used to characterize workload concentration and regime structure at the handshake level. They are not intended as substitutes for full function tracing, fine-grained call-path reconstruction, or provider-internal attribution. Their role is to support causal interpretation at the level of client/server burden rather than to provide exhaustive implementation forensics.